The UARS and EOS Microwave Limb Sounder (MLS) experiments

J.W. Waters, W.G. Read, I.. Froidevaux, R.F. Jarnot, R.E. Cofield, D.A. Flower, G.K. Lau, H.M. Pickett, M.L. Santee, D.L. Wu, M.A. Boyles, J.R. Burke, R.R. Lay, M.S. Loo, N.J. Livesey, T.A. Lungu, G.L. Manney, L.L. Nakarnura, V.S. Perun, B.P. Ridenoure, Z. Shippony, P.H. Siegel, R.P. Thurstans

California Institute of Technology Jet Propulsion Laboratory, Pasadena CA 91109, USA

R.S. Hat-wood, H.C. Pumphrey, M.J. Filipiak

Edinburgh University Dept. of Meteorology, Edinburgh ScotlandEH93JZ, UK

submitted to
Journal of the Atmospheric Sciences

special issue on
Global Measurement Systems for Atmospheric Composition
(IGAC SPARC GAW conference held 20-22 May 1997 in Toronto, Canada)

ABSTRACT

The Microwave Limb Sounder (MLS) experiments obtain measurements of atmospheric composition, temperature and pressure by observations of millimeter and submillimeter-wavelength thermal emission as the instrument field-of-view is scanned through the atmospheric limb. Features of the measurement technique include the ability to provide global coverage on a daily basis at all times of day and night from an orbiting platform, to obtain reliable measurements even in the presence of dense cirrus and aerosol, and to measure many atmospheric gases as well as temperature and pressure. The composition measurements are relatively insensitive to uncertainties in atmospheric temperature. An accurate spectroscopic data base is available, and the instrument calibration is also very accurate and stable. The first MLS experiment in space, launched on the NASA Upper Atmosphere Research Satellite (UARS) in September 1991, was designed primarily to measure stratospheric profiles of ClO, 0_3, H_20 and atmospheric pressure as a vertical reference. Global measurement of C1O, the dominant radical in chlorine destruction of ozone, was an especially important objective of UARS MLS. All objectives of UARS MLS have been accomplished, and additional geophysical products beyond those for which the experiment was designed have been obtained. A follow-on MLS experiment is being developed for NASA's Earth Observing System (EOS), and scheduled to be launched on the EOS CHEM platform in 2002. EOS MLS is designed for many stratospheric measurements, including HO_x radicals which could not be measured by UARS because adequate technology was not available, and better and more extensive upper tropospheric and lower stratospheric measurements.

1. Introduction

Microwave limb sounding obtains remote measurements of atmospheric parameters by observations of millimeter and submillimeter-wavelength thermal emission as the instrument field-of-view (FOV) is scanned through the atmospheric limb from above. Development of the MLS experiments began at the Jet Propulsion Laboratory in the mid-1970's and included instruments deployed on aircraft (Waters et al. 1979, 1980) and balloon (Waters et al. 1981, 1984, 1988; Stachnik et al. 1992) prior to application of the technique from space. The measurement technique is described by Waters (1989; 1992a,b; 1993). Its features include: (1) the ability to measure many atmospheric gases, with emission from molecular oxygen providing temperature and pressure; (2) measurements that can be made reliably, even in the presence of heavy aerosol, dense cirrus or polar stratospheric clouds which can degrade ultraviolet, visible and infrared techniques; (3) the ability to make measurements at all times of day and night and provide global coverage on a daily basis; (4) the ability to spectral] y-resolve emission lines at all altitudes, which allows measurements of very weak lines in the presence of nearby strong ones; (5) composition measurements that are very insensitive to uncertainties in atmospheric temperature; (6) a very accurate spectroscopic data base; and (7) instrumentation that has very accurate and stable calibration, adequate sensitivity without necessarily requiring cooling, can be modularly designed for accommodating changing measurement priorities and provides good vertical resolution set by size of the antenna. New miniature integrated circuit technology for microwave radiometers (Weinreb 1997), now being studied for use in a future experiment, can provide good horizontal resolution (including complete coverage between orbits) by allowing an array of radiometers with multiple FOVS simultaneously scanning the limb at different azimuth angles (Waters 1997a).

Spectral line frequencies and strengths used for interpreting the MLS atmospheric measurements are obtained from the JPL *Submillimeter, Millimeter, and Microwave Spectral Line Catalog* (Pickett et al. 1992). Accuracy of line frequencies is typically seven digits or more, and of line strengths is typically 4 digits. The catalog data base is searched to ensure that all gases which might contribute significant amounts to the MLS signals are included in the data processing. Line-broadening parameters are obtained from laboratory measurements, e.g., Pickett et al. (1981) and Oh and Cohen (1992, 1994), with uncertainties of-30A.

2. The UARS Microwave Limb Sounder

a. Some general information on UARS MLS

The MLS launched 12 September 199 I on the Upper Atmosphere Research Satellite (e.g., Reber 1993; Reber et al. 1993; Waters 1997b) is the first application of the microwave limb sounding technique from space. A

somewhat similar experiment, the Millimeter-wave Atmospheric Sounder (MAS) has been flown on three Space Shuttle missions (Hartmann et al. 1996). The UARS MLS development was led by the California Institute of Technology Jet Propulsion Laboratory, with collaboration from Rutherford Appleton Laboratory, Heriot-Watt University, and Edinburgh University in the United Kingdom. The instrument (Barath et al. 1993) contains ambient-temperature heterodyne radiometers that operate near 63 GHz (designed to measure stratospheric pressure, but also provides stratospheric temperature); 205 GHz (designed to measure stratospheric ClO, 0_3 and H_20_2); and 183 GHz (designed to measure stratospheric and mesospheric H_20 and 03). Figure 1 shows a signal flow block diagram. Calibration of UARS MLS, described by Jarnot et al, (1996), is accurate to -3% (3σ) overall in the most critical spectral bands. Lau et al. (1996) analyze the low-frequency 1/f noise of the instrument.

Figure 2 shows an example of spectra measured by MLS, and illustrates its ability to spectrally-resolve individual emission lines. Having several spectral channels covering a single emission line, and resolving this line at all altitudes of interest, provides robust measurements since geophysical quantities can usually be obtained from the channel-to-channel spectral ly-varying component of the measured thermal emission. Extraneous effects, such as stray radiation, generally have spectrally-flat emission over the spectral range used for measurements, and their uncertainties do not usually have first-order effects on the retrievals of geophysical parameters. Figure 3 shows 205 GHz radiances from the lower stratosphere measured by UARS MLS when the tropics contained very heavy loading of aerosol from the Mt. Pinatubo volcano. No effect of the aerosol on the MLS radiances is seen, as expected from theoretical considerations, with an observed upper limit of ~0.1%.

Validation of the MLS primary data products, and their accuracies and precision, are described in the ***Journal of Geophysical Research*** special issue (volume 101, number D6, 30 April 1996) on UARS data evaluation: temperature/pressure by Fishbein et al. (1996); 0_3 by Froidevaux et al. (1996), Cunnold et al. (1996a,b), and Ricaud et al. (1996); H_2O by Lahoz et al. (1996a); ClO by Waters et al. (1996). Figure 4 shows the agreement obtained between MLS and some other well-calibrated measurements of the stratospheric 0_3 profile. Additional results relevant to validation of these MLS measurements are included inAelligetal.(1996), Crewell et al. (1995), Redaelli et al. (1994), Singh et al. (1996) and Wild et al. (1995). Although MLS was designed to include measurement of H_20_2, this measurement was predicated on stratospheric H_20_2 being a major odd-hydrogen reservoir in the middle stratosphere with predicted abundances of-1 O parts per billion by volume (ppbv). Refinements to parameters used for the theoretical predictions, and measurements (e.g., Chance et al. 1991), now indicate only -0.1 ppbv H_20_2 in the stratosphere; preliminary detection of a signal, corresponding to -O. 1 ppbv H_20_2 has been obtained in averages of the MLS radiances (unpublished results). Additional data products obtained from UARS MLS, beyond that for which the instrument was primarily designed, include $S0_2$ injected into the stratosphere by the Pinatubo volcano (Read et al. 1993), upper

tropospheric H_2O (Read et al. 1995), lower stratospheric HNO_3 (Santee et al. 1995, 1996a, 1997 b), temperature variances associated with atmospheric gravity waves in the stratosphere and mesosphere (Wu and Waters 1996a,b; 1997), and ice content of cirrus (D.L. Wu, manuscript in preparation). Fourier-transform techniques applied to mapping MLS data are described by Elson and Froidevaux (1993). Figure 5 shows the vertical range of measurements obtained to date from the UARS MLS experiment.

UARS was designed for an 18-month duration mission, but at the time of writing, MLS (along with most other UARS instruments) continues to operate after nearly 6 years in orbit with no degradation in its 63 and 205 GHz measurements except for time-sharing of these measurements with those of other UARS instruments due to decreases in power available from the spacecraft. The MLS 183 GHz measurements ceased in April 1993 after 18 months of excellent data had been obtained. Updated information can be obtained from the MLS web site home page (http: //mls.jpl.nasa.gov).

b. UARS MLS results related to ozone loss in polar regions

Early results from UARS MLS included the first maps of stratospheric C1O, the predominant form of chemically-reactive chlorine involved in the destruction of stratospheric 0_3, throughout the winter vortices of both the Antarctic and Arctic. Initial results (Waters et al. 1993a,b; see also Chipperfield 1993) showed the lower stratospheric Antarctic vortex to be filled with ClO in the region where 0_3 was depleted, confirming earlier conclusions from ground-based and aircraft instruments that chlorine chemistry is the cause of the Antarctic ozone hole. They showed (Figure 6) that C1O in the sunlit portion of the Antarctic vortex can become enhanced by June, and that O_3 destruction by ClO is masked in the early Antarctic winter by influx of 0_3 expected from diabatic descent. Enhanced C1O in the Antarctic vortex has been observed by MLS as early as late May to mid June in each of its six years of operation to date; Figure 7 shows maps for the earliest day each year when enhanced Antarctic ClO was observed by MLS. Recent analyses (Roscoe et al. 1997) of ground-based measurements and models also show evidence of Antarctic ozone loss starting in midwinter. Early MIS results also showed (Figure 8) that the Arctic winter lower stratospheric vortex can become filled with enhanced ClO, corresponding to calculated vortex-averaged 0_3 destruction rates of ~0.7% per day. Results from 3D models (Douglass et al. 1993; Geller et al. 1993; Lefevre et al. 1994), produced shortly after the MLS results were obtained, showed the observed distribution and evolution of enhanced Arctic C1O were consistent with chemical-transport model predictions. The maximum ClO abundances from MLS, however, are slightly larger than predicted from the models (Lefevre et al. 1994; Lutman et al. 1997). A clear relationship was found between enhanced Arctic ClO observed by MLS and predicted polar stratospheric cloud formation along back trajectories associated with the enhanced ClO; sporadic large values of ClO seen by MLS outside the vortex were shown to be consistent with that expected to be caused by instrument noise (Schoeberl et al. 1993). Differences between the Arctic and Antarctic winter vortex conditions deduced from MLS observations are described by Santee et al. (1995), and deduced from combined MLS, CLAES (Cryogenic

Limb Array EtaIon Spectrometer) and HALOE (Halogen Occultation Experiment) data by Douglass et al. (1995). One difference between the Arctic and Antarctic is the decreased amount of HNO_3 in the Antarctic winter vortex relative to the Arctic, as shown in Figure 9. $HN0_3$ provides a source of NO_x which quenches reactive chlorine and the depletion of HNO_3 over Antarctica leads to extended depletion of 0_3 there. The smaller Antarctic abundances of $HN0_3$ can be traced to the lower temperatures and their longer duration in the Antarctic where polar stratospheric cloud particles containing $HN0_3$ can sediment out of the stratosphere. A major question for future Arctic ozone loss is the extent to which the decrease in Arctic lower stratospheric temperatures, possibly expected from increasing greenhouse gases, will lead to more Arctic ozone loss (due to strong non-linear temperature-dependence of the responsible mechanisms) even though stratospheric chlorine abundances should slowly start decreasing with the cease in industrial production of source gases. Analyses of MLS $HN0_3$ observations through several Antarctic winters (Santee et al. 1997b) have provided implications for processes related to formation of polar stratospheric clouds; and indicate that ternary solutions (Tabazadeh et al. 1994) play an important role. Analyses by Massie et al. (1997) of MLS, CLAES and ISAMS measurements over Scandinavia during 9-10 January 1991 imply initial PSC growth processes which transform sulfate droplets into ternary droplets or nitric acid dihydrate particles.

Definitive loss of Arctic ozone due to chemistry associated with the enhanced ClO was determined from analyses of combined MLS and UARS CLAES data by Manney et al. (1994). Bell et al. (1994) found the expected anticorrelation between enhanced Arctic ClO measured by MLS and HCl measured from the ground. Additional confirmation of the paradigm of chemical processing by polar stratospheric clouds leading to activation of stratospheric chlorine is shown in the analyses of northern hemisphere CLAES, MLS and HALOE data by Geller et al. (1995), and in southern hemisphere MLS and CLAES data by Ricaud et al. (1995). Mackenzie et al. (1996) compare lower stratospheric vortex ozone destruction calculated from the MLS ClO with the MLS-observed change in 0_3 for the northern winter of 1992-93 and southern winter of 1993. Additional comparisons between MLS observations and model results for polar chemistry are given by Eckman et al. (1995), Chipperfield et al. (1 996) and Santee et al. (1996a). Schoeberl et al. (1 996) use MLS, HALOE and CLAES data in an analysis of the development of the Antarctic ozone hole. MLS measurements of Arctic C1O and 0_3 for the six northern winters observed to date are described in the collective papers of Manney et al. (1994; 1995a,b; 1996a,b; 1997a), Santee et al. (1995, 1996b, 1997b) and Waters et al. (1993a,b; 1995). The largest vortex-averaged abundances of ClO in the Arctic and the largest Arctic ozone loss observed to date by MLS occurred in the 1995-96 winter (Manney et al. 1996b, 1997a; Santee et al. 1996b, 1997a). Filling, or near-filling, of the Arctic lower stratospheric winter vortex with enhanced ClO abundances has been seen in each northern winter of MLS observations; and Figure 10 shows measurements in the 1996 and 1997 winters. Low ozone "pockets" in the middle stratospheric winter anticyclone have also been observed in MLS data and analyzed by Manney et al. (1995c), who show these cannot be explained solely by transport.

c. UARS MLS results related to high latitude atmospheric dynamics

MLS observations have been used in several studies to provide information on vortex and high-latitude dynamics, Harwood et al. (1993) studied the effects of the break-up of the Antarctic vortex on the water vapor distribution during September and November 1991 and, among other things, showed large parcels of air from the Antarctic vortex migrating to midlatitudes (Figure 11). Manney et al. (1993) describe the evolution of ozone observed by MLS in relation to the Antarctic polar vortex in August and September 1992, and Fishbein et al. (1993) analyzed waves seen in MLS observations of stratospheric temperature and ozone during this period. Lahoz et al. (1993, 1994) use MLS H_20, CLAES N_20 and UK Meteorological Office data to study the evolution of mid-stratospheric water vapor and vortex processes in the northern hemisphere winter of 199 1-92; Lahoz et al. (1996b) do a similar study for the southern hemisphere winter of 1992. Manney et al. (1995d,e) compare Lagrangian transport calculations with MLS observations of H_20 and 0_3, and CLAES observations of N_20 and CH_4. Morris et al. (1995) apply a trajectory mapping technique to compare MLS and HALOE water vapor measurements and analyze dynamical wave-breaking events. Orsolini et al. (1997) and Manney et al. (1997b) use MLS O_3 data to initialize a high-resolution transport model and analyze ozone laminae along the Arctic polar vortex edge seen in lidar and ozonesonde data.

d. UARS MLS results related to global distributions and variations of atmospheric parameters

An overview of zonal mean O_3 results from the first two and one-half years of MLS operation is given by Froidevaux et al. (1994); in addition to features observed in stratospheric O_3, this work includes initial results of examining residual differences between the stratospheric 0_3 column from MLS and the total 0_3 column from TOMS, with information on tropospheric ozone as the ultimate goal. Analyses by Ziemke et al, (1996) using these data sets have shown zonal asymmetries in southern hemisphere column ozone that have implications of biomass burning. Elson et al. (1994) describe large-scale variations observed in MLS 0_3, and Elson et al. (1996) show zonal and large-scale variations in MLS H_2O. Pumphrey andHarwood(1997) analyze MLS radiance data to obtain information on variations of H_20 and 0_3 throughout the mesosphere, and show that H_20 in the mesosphere is transported mainly by advection; future processing of MLS data will use non-linear retrieval algorithms for H_20 which should improve the standard MLS H_20 product in the mesosphere and elsewhere (Pumphrey 1997). Randel et al. (1995) include MLS and HALOE data in analyzing changes in stratospheric ozone following the Pinatubo eruption. Dessler et al. (1995) found that incorporation of 0_3 measured by MLS into chemical relationships improved comparison between predicted correlations of HCl and $C10N0_2$ and those measured by HALOE and CLAES. Chandra et al. (1996) use MLS data in examining ozone variability in the upper stratosphere during the declining phase of solar cycle 22.

The zonal mean latitudinal distribution of ClO observed by MLS in the upper stratosphere (Figure 12; see also Waters et al, 1996, and Jackman et al. 1996) shows a minimum at low latitudes as expected (Solomon and Garcia, 1984) from increased quenching by larger amounts of upper stratospheric CH_4 at low latitudes which is due to rising motion in the tropics transporting CH_4 from lower altitudes. As shown in Figure 12, the upper stratospheric ClO minimum moves northward in northern summer qualitatively tracking the seasonal variation in CH_4 (Kumer et al. 1993) which follows the rising motion in the tropics. Explanation of the -0.1 ppbv difference in upper stratospheric ClO for the two periods shown here is under investigation. Eckman et al. (1995) found that quantitative agreement of theoretical model predictions with MLS upper stratospheric C1O measurements is substantially improved by including 5% branching of the reaction OH+ClO to $HCl+O_2$, consistent with a conclusion on this reaction reached earlier by Toumi and Bekki (1993) in regards to matching the Submillimeter Limb Sounder (S1.S) measurements of upper stratospheric ClO and HCl (Stachnik et al. 1992). Dessler et al. (1996a) used MLS ClO measurements, along with CLAES $ClONO_2$ and HALOE $N0_2$, to test predictions of chlorine partitioning between ClO and $ClONO_2$. Dessler et al. (1996b) also used MLS ClO, and HALOE and CLAES $N0_2$, to examine implications for the model "ozone deficit" in the upper stratosphere. An increasing trend in upper stratospheric ClO, expected from increasing abundances of stratospheric chlorine, and a decreasing trend in lower stratospheric C1O, expected from changes in heterogeneous chemistry during the fallout of Pinatubo aerosols, has been detected in MLS data (L. Froidevaux, manuscript in preparation), with some results shown in Figure 13.

Two-day waves in the stratosphere have been analyzed by Limpasuvan and Leovy (1 995) using MLS H_2O data, and by Wu et al. (1996) using MLS temperatures. Four-day waves observed in MLS ozone, temperature and geopotential height have been analyzed by Allen et al. (1997). MLS data have been used in calculations of stratospheric residual circulation by Rosenlof (1 995) and Eluszkiewicz et al. (1996). Synopic-scale features have been observed in MLS upper tropospheric H_20; one observed over the east coast of the US during March 1993 has been compared with independent results from the Goddard Space Flight Center data assimilation model, and good qualitative agreement obtained (Read et al. 1995). Stone et al. (1996) used MLS upper tropospheric H_20 measurements to investigate the structure and evolution of eastward-traveling medium-scale wave features in the southern hemisphere summertime; they found results consistent with paradigms for the structure and evolution of baroclinic disturbances.

e. UARS MLS results related to the tropics

Kelvin waves observed in MLS tropical data have been analyzed by Canziani et al. (1994, 1995) and Stone et al. (1995), and MLS observations of the semiannual oscillation have been analyzed by Ray et al. (1994). Randel et al. (1993) describe CLAES and MLS observations of stratospheric transport from the tropics to middle latitudes by planetary wave mixing. Carr et al. (1995) performed initial analyses of MLS tropical stratospheric $}1_20$ data, and Mote et al. (1995) found variations in these data that could be related to the annual

cycle in tropical tropopause temperatures. More extensive analyses by Mote et al. (1996), aided by the use of UARS Halogen Occultation Experiment (HALOE) H_20 and CH_4, confirmed that tropical air entering the stratosphere from below is marked by its tropopause water vapor mixing ratio and retains a distinct memory of tropical tropopause conditions for 18 months or more; this analysis implies that vertical mixing is weak and that subtropical stratospheric "transport barriers" are effective at inhibiting transport into the tropics. Schoeberl et al. (1997) also use MLS and other UARS data to estimate the dynamical isolation of the tropical lower stratosphere. Preliminary MLS upper tropospheric H_2O is reasonably consistent with NASA ER-2 aircraft measurements (Newell et al. 1996a), and with the expected tropical Walker circulation (Newell et al. 1996b). Newell et al. (1997) found variations in MLS tropical upper tropospheric H_2O over the 1991-1994 period to be closely related to sea surface temperature variations in the eastern tropical Pacific, at both seasonal and interannual time scales. Figure 14 shows variations observed in MLS upper tropospheric H_20 over the tropical Pacific for all measurements made to date; good correlation is obtained with the occurrence of El Nino events. A new product recently been obtained from MLS is the ice content of cirrus in the upper troposphere (D.L. Wu et al., manuscript in preparation), and Figure 15 gives preliminary results which show largest ice abundances associated with regions of greatest convection in the tropics, as expected. Because its observation wavelengths are much larger than the cirrus particles, the MLS signal from cirrus is dependent to first order upon the total ice content and is relatively insensitive to the cirrus particle size distribution. MLS measurements can be thus be reported as ice content, which cannot be done directly for infrared and visible measurements where cirrus observations are typically reported as extinction coefficients at the observation wavelengths.

f. UARS MLS results for atmospheric gravity waves

Analyses of the 63 GHz radiances from MLS have produced the first global maps of atmospheric temperature variances at -100 km horizontal scales associated with gravity wave activity in the stratosphere and mesosphere (Wu and Waters 1996a,b; 1997). These data provide information on gravity waves with spatial scales of-30- 100 km in the horizontal and -10 km in the vertical. The mapped variances show high correlation with regions of strong background winds that are expected to play a major role in determining gravity wave amplitudes in the stratosphere and mesosphere. The observed variance grows exponentially with height in the stratosphere, and saturates in the mesosphere as expected from wave breaking and dissipation at the higher altitudes. The data also show correlation with surface topography features and regions of tropospheric convective activity, which are expected sources of gravity waves. Analysis by Alexander (1997) indicates that the MLS maps are consistent with model predictions of atmospheric gravity wave behavior but that the dominant patterns in the maps can be explained by the Doppler-shifting effects of background winds on the gravity wave spectrum, without requiring any geographical variation in the sources. The extent to which MLS can provide information on atmospheric gravity wave sources is a current topic of investigation.

g. UARS MLS results for SO_2 injected into the stratosphere by volcanoes

Starting within 10 days of launch, and continuing for approximately 2 months, MLS observed the 3-dimensional distribution and decay of residual SO_2 injected into the tropical stratosphere by the Mt. Pinatubo eruption that occurred about 3 months before launch of UARS. These observations (Read et al. 1993) showed the Pinatubo SO_2 mixing ratio maximum to occur around 26 km altitude with abundances of-15 ppbv on 21 September 1991. The observed SO_2 decay has e-folding times of 29 days at 26 km and41 daysat21 km, consistent with expectations that the primary destruction of SO_2 is due to reaction with OH leading to formation of stratospheric sulfate aerosols. Projected backward to time of eruption, the total amount of SO_2 injected by Pinatubo is estimated from MLS data to be 17 Mtons, consistent with estimates inferred from other measurements. SO_2 injected into the stratosphere by the South American Lascar volcano was also detected by MLS on 21 and 22 April 1993 (unpublished results).

3. **The Earth Observing System (EOS) MLS**

a. Some general information on EOS MLS

EOS MLS will be improved over UARS MLS in providing(1) additional stratospheric measurements for chemical composition and long-lived dynamical tracers, (2) more upper tropospheric measurements, (3) better global coverage, and (4) better precision and spatial resolution. These improvements are possible because of (1) advances in microwave technology since UARS MLS, (2) a better understanding of the capabilities of the measurement technique as a result of the UARS experience, and (3) the EOS near-polar orbit which allows nearly pole-to-pole coverage on each orbit, whereas the UARS orbit (inclined 57 degrees to the equator) and its precession forces MLS to switch between northern and southern high latitude measurements on an approximate monthly basis and critical periods are often missed. EOS MLS observes in the orbital plane (looking forward) which provides latitude coverage between 82° S and 82° N on each orbit.

EOS MLS has radiometers which operate in spectral bands centered near 120, 190, 240, 640 and 2500 GHz. All radiometers are planned to incorporate advanced technology including planar-technology mixers (Siegel et al. 1993), and integrated circuit radiometers (Weinreb et al. 1997) at 120 GHz. Figure 16 shows a signal flow block diagram for EOS MLS, and Figure 17 shows the spectral bands it measures, Vertical resolution of the EOS MLS measurements is generally -2-3 km (about 2x better than UARS MLS), although this will vary depending upon signal-to-noise for the particular measurement, and there are trade-offs between vertical

resolution and precision. Each EOS MLS limb scan, under nominal operation, will be performed approximately every 1.5 degrees great circle along the orbital track (about 170 km distance and 25 s in time), which is -3x more dense than on UARS MLS. The nominal scan range will be from -2 km to -60 km above Earth's surface. However, the vertical scan is programmable and alternative scan patterns can be chosen to provide more intense measurements of certain altitude regions or to provide measurements at higher altitudes in the mesosphere and lower thermosphere. Figure 18 shows the suite of measurements planned from each of the EOS MLS radiometers.

b. EOS MLS measurements for stratospheric chemistry

EOS MLS will provide key measurements throughout the stratosphere to test our understanding of its them istry, and provide new insights and early detection of changes. The lower stratospheric measurements are particularly important since they will occur when (1) lower stratospheric ozone, especially in the Arctic, is vulnerable to increased depletion due to effects of small decreases in temperature and potential changes in other parameters such as an increase in H_20, (2) stratospheric chlorine loading is at or near its maximum, and (3) some recovery of ozone at low altitudes in the Antarctic ozone hole might be detectable in the later portion of the mission (Hofmann)996) to verify that CFC regulations are having the expected effect.

The simultaneous and commonly-calibrated MLS measurements of ClO, $HN0_3$, H_20, HCl, N_20, 0_3 and temperature provide a powerful suite to improve understanding of key processes which "could lead to massive ozone loss in the Arctic and provide diagnostics of the loss. C1O abundances allow estimates of the amount of ozone loss due to chlorine chemistry. Abundances of HNO_3 and H_20, and temperature, critically affect the microphysics leading to formation of surfaces upon which heterogeneous chemistry can occur and convert chlorine from reservoir to reactive forms. Abundances of $HN0_3$ also affect the rate at which reactive chlorine is converted back to reservoir forms. Measurements of N_20, a long-lived tracer, help separate chemical and dynamical causes of observed changes. Measurements of OH, $H0_2$, BrO, and HOCl, along with those mentioned above, will improve our understanding of tropical and mid-latitude stratospheric ozone changes. The suite of measurements includes key species in the HO_x and ClO_x cycles now thought to dominate tropical and mid-latitude lower stratospheric ozone loss. The ability of MLS to observe through dense aerosol will be critical for monitoring stratospheric chemistry after any volcanic eruptions which cause large increases in stratospheric aerosol loading.

The EOS MLS measurements of stratospheric OH will fill a serious gap in global observations to date because, as stated in the report of a Workshop on Atmospheric Trace Gas Measurements for the Year 2000 and Beyond published in the January/February 1995 issue of the EOS publication ***The Earth Observer, (1) OH*** controls the conversion of CH_4 to H_20, (2) reactions oft IO_x radicals are the most important loss mechanisms for ozone in both the lowest and highest regions of the stratosphere, (3) reactions with011 control the rate of oxidation of

sulfur gases (SO_2, OCS) to sulfate aerosol, and (4) OH is in competition with heterogeneous chemistry in controlling the transfers between radical species in both the NO_y and Cl_x systems. 'OH may be a well-behaved constituent under a wide range of circumstances, as must be assumed in models in absence of measurements to the contrary, but it is essential that this assumption be tested.'

The good simultaneous measurements of H_2O, cirrus ice content, temperature, O_3, CO, and N_2O in the region of the tropopause should improve our understanding of exchange processes between the stratosphere and troposphere. The MLS measurements are especially important in the tropics where they can be made in the presence of dense cirrus which can degrade techniques operating at ultraviolet, visible and infrared wavelengths.

c. EOS MLS measurements for upper tropospheric chemistry

EOS measurements in the upper troposphere include H_2O, O_3, CO, N_2O, HCl, ice content of dense cirrus, temperature and pressure. The simultaneous measurement of O_3 and CO, which serves as a tracer of air mass origin and motion, should provide new information on the global distribution, variation and sources of O_3 in the upper troposphere. Some of the larger variations expected in upper tropospheric O_3 and CO due to biomass burning (e.g., Thompson et al. 1996; Pickering et al. 1996) should be detectable in daily maps from EOS MLS but smaller variations will require maps built up from averages of observations over a longer period of time. Improvements in the MLS ability to measure stratospheric ozone column will lead to improved determinations of tropospheric ozone obtained from residuals between total column ozone measured by other sensors and the stratospheric column from EOS Ml .S.

Pronounced minima in upper tropospheric O_3 in the presence of ice clouds have been detected by ground-based lidar (Reichardt et al. 1996). These low values of ozone can possibly be explained by heterogeneous chemistry on cirrus cloud particles activating chlorine (Reichardt et al. 1996, Borrmann et al. 1996; Solomon et al. 1997). EOS MLS will help understand such phenomena on a global scale since it concurrently measures O_3 and cirrus ice, as well as CO which can likely help identify regions of convective uplift where low O_3 might be due to dynamics and N_2O and HCl which can help identify air of stratospheric origin and provide estimates of the amount of inorganic chlorine available for activation by heterogeneous chemistry.

d. EOS MLS measurements for climate variability studies

EOS MLS measurements relevant to climate variability studies include H_2O, cloud ice content, temperature and O_3. The MLS measurements of H_2O in the upper troposphere are expected to be especially valuable because of uncertainties in climate feedback mechanisms associated with upper tropospheric H_2O (e.g., Lindzen 1990), and the ability of MLS to provide such measurements in the presence of cirrus and with good vertical resolution. Some of the more interesting phenomena related to climate variability and feedback are

associated with the behavior of upper tropospheric water vapor in and around regions of deep convection in the tropics where the presence of cirrus can degrade measurements by shorter-wavelength techniques. The simultaneous MLS measurements of water in both the vapor and ice phases, along with temperature (and CO as a possible tracer of air motion), should provide new information on processes which affect formation of cirrus ice particles which can have important climatic effects. The MLS temperature measurements complement those from infrared techniques in not being affected by variations in stratospheric aerosol content or $C0_2$, and complement those from nadir-looking microwave techniques in having better vertical (but poorer horizontal) resolution.

ACKNOWLEDGMENTS

We thank many colleagues on the MLS team, too numerous to mention here by name, who have contributed so much to our experiments. Special thanks are due F.T. Barath for managing the UARS MLS instrument development, M.A. Frerking for leading the development of its JPL radiometers, and G.E. Peckham and colleagues involved with the UK portion of the instrument. Thanks also to E.A. Cohen and colleagues for laboratory spectroscopy support, and R.E. Newell, R.J. Salawitch and M.R. Schoeberl for many helpful discussions. This work was performed at the California Institute of Technology Jet Propulsion Laboratory under contract with the U.S. National Aeronautics and Space Administration and at the University of Edinburgh Department of Meteorology under contract with the U.K. National Environmental Research Council.

REFERENCES

Aellig, C. P., N. Kämpfer, C. Rudin, R. M. Bevilacqua, W. Degenhardt, P. Hartogh, C. Jarchow, K. Künzi, J. J. Olivero, C. Croskey, J. W. Waters, and H. A. Michelsen, 1996: Latitudinal distribution of upper stratospheric ClO as derived from space borne microwave spectroscopy, *Geophys. Res. Lett.,* 23, 2321-2324.

Alexander, M. J., 1997: A model of non-stationary gravity waves in the stratosphere and comparison to observations, 'in *Gravity Wave Processes and Their Parameterization in Global Climate Models,* edited by K. Hamilton, vol. 50, pp. 153-168. Springler-Verlag NATO ASI Series 1, Ncw York.

Allen, D. R., J. L. Stanford, L. S. Elson, E. F. Fishbein, I,. Froidevaux, and J. W. Waters, 1997: The 4-day wave as observed from the Upper Atmosphere Research Satellite Microwave Limb Sounder, *J. Atmos. Sci.,* 54, 420 434.

Barath, F. T., M. C. Chavez, R. E. Cofield, D. A. Flower, M. A. Frerking, M. B. Gram, W. M. Harris, J. R. Holden, R. F. Jarnot, W. G. Kloczeman, G. J. Klose, G. K. Lau, M. S. Loo, B. J. Maddison, R. J. Mattauch, R. P. McKinncy, G. E. Peckham, H. M. Pickett, G. Siebes, F. S. Soltis, R. A. Suttie, J. A. Tarsala, J. W. Waters, and W. J. Wilson, 1993: The Upper Atmosphere Research Satellite Microwave Limb Sounder Instrument, *J. Geophys. Res.*, 98, 10,751-10,762.

Bell, W., N. A. Martin, T. D. Gardiner, N. R. Swarm, P. T. Woods, I'. F. Fogal, and J. W. Waters, 1994: Column measurements of stratospheric trace species over Åre, Sweden in the winter of 1991-92, *Geophys. Res. Lett.*, **21**, 1347-1350.

Borrman, S., S. Solomon, J. E. Dye, and B. Luo, 1996: The potential of cirrus clouds for heterogeneous chlorine activation, *Geophys. Res. Lett.*, 23, 2133 2136.

Canziani, P. O., J. R. Holton, E. F. Fishbein, L. Froidevaux, and J. W. Waters, 1994: Equatorial Kelvin Waves: A UARS MLS View: *Journal of Atmos Sci. (special issue on UARS early scientific results),* **51**, 3053 3076.

, - , - , and -, 1995: Equatorial Kelvin wave variability during 1992 and 1993, *J. Geophys. Res.,* 100, 51935202.

Carr, E. S., R. S. Harwood, P. W. Mote, G. E. Peckham, R. A. Suttic, W. A. Lahoz, A. O'Neill, L. Froidevaux, R. F. Jarnot, W. G. Read, J. W. Waters, and R. Swinbank, 1995: Tropical st ratosphcric water vapor measured by the microwave limb sounder (MI, S), *Geophys. Res. Lett.*, 22, 691 694.

Chance, K. V., D. G. Johnson, W. A. Traub, and K. W. Jucks, 1991: Measurements of the stratospheric hydrogen peroxide profile using far infrared thermal emission spect roscopy, *Geophys. Res. Le.?t.,* 18, 1003 1006.

Chandra, S., I,. Froidevaux, J. W. Waters, O. R. White, G. J. Rottman, D. K. Prinz, J. W. Waters, and G. E. Brueckner, 1996: Ozone variability in the upper stratosphere during the declining phase of solar cycle **22**, *Geophys. Res. Lett.*, 23, 2935 2938.

Chipperfield, M., 1993: Satellite maps ozone destroyer, *Nature*, 362, 592 593.

, M. L. Santee, L. Froidevaux, G. L. Manney, W. G. Read, J. W. Waters, A. E. Roche, and J. M. Russell, 1996:

Analyses of UARS data in the southern polar vortex in September 1992 using a chemical transport model, *J. Geophys. Res.*, 101, 18,861-18,881.

Crewell, S., R. Fabian, K. Künzi, H. Nett, T. Wehr, W. Read, and J. Waters, 1995: Comparison of ClO measurements made by airborne and spaceborne microwave radiometers in the Arctic winter stratosphere 1993, *Geophys. Res. Lett.*, *22, 1489 1492.*

Cunnold, D., H. Wang, W. P. Chu, and L. Froidevaux, 1996a: Comparisons between Stratospheric Aerosol and Gas Experiment 11 and microwave limb sounder ozone measurements and aliasing of SAGE 11 ozone trends in the lower stratosphere, *J. Geophys. Res.*, 101, 10,061-10,075.

, L. Froidevaux, J. M. Russell, B. Connor, and A. Roche, 1996b: Overview of UARS ozone validation based primarily on intercomparisons among UARS and Stratospheric Aerosol and Gas Experiment II measurements, *J. Geophys. Res.*, 101, 10,335 10,350.

Dessler, A. ?3., D. B. Considine, G. A. Morris, M. R. Schoeberl, A. E. Roche, , J. Mergenthaler, J. M. Russell, J. W. Waters, J. Gille, and G. K. Yue, 1995: Correlated observations of HCl and $ClONO_2$ from UARS and implications for stratospheric chlorine partitioning, *Geophys. Res. Lett.*, 22, 1721-1724,

, S. R. Kawa, A. Douglass, D. B. Considine, J. B. Kumer, A. E. Roche, J. W. Waters, J. M. Russell 111, and J. C. Gille, 1996a: A test of the partitioning between ClO and $ClONO_2$ using simultaneous UARS measurements of (30, NO_2 and C1ONO2, *J. Geophys. Res.*, **101**, 12,515 12,521.

, S. R. Kawa, D. B. Considine, J. W. Waters, L. Froidevaux, and J. B. Kumer, 1996b: UARS measurements of ClO and NO_2 at 40 and 46 km and implications for the 'ozone deficit', *Geophys. Res. Lett.*, 23, 339-342.

Douglass, A., R. Rood, J. Waters, L. Froidevaux, W. Read, L. Elson, M. Geller, Y. Chi, M. Cerniglia, and S. Steenrod, 1993: A 3D simulation of the early winter distribution of reactive chlorine in the north polar vortex, *Geophys. Res. Lett.*, 20, 1271-1274.

, M. R. Schoeberl, R. S. Stolarski, J. W. Waters, J. M. Russell III, and A. E. Roche, 1995: Interhemispheric differences in springtime production of HCl and $ClONO_2$ in the polar vortices, *J. Geophys. Res.*, 100, 13,967-13,978.

Eckman, R. S., W. L. Grose, R. E. Turner, W. T. Blackshear, J. M. Russell 111, L. Froidevaux, J. W. Waters, J. I?. Kumer, and A. E. Roche, 1995: St ratospheric trace const it uents simulated by a three-dimensional general circulation model: Comparison with UARS data, *J. Geophys. Res.*, 100, 13,951–13,966.

Elson, L. S., and I,. Froidevaux, 1993: The usc of Fourier transforms for asynoptic mapping: Early results from t hc Upper Atmosphere Research Satellite Microwave Limb Sounder, *J. Geophys. Res.*, 98, 23,039 23,049.

, G. L. Manney, L. Froidevaux, and J. W. Waters, 1994: Large-scale variations in ozone from the first two years of UARS MLS data, *Journal of Atmos Sci. (special issue on UARS early scientific results), 51, 2867* 2876.

, W. G. Read, J. W. Waters, P. W. Mote, J. S. Kinnersley, and IL S. Harwood, 1996: Space-tirrm variations in

water vapor as observed by the UARS Microwave Limb Sounder, *J. Geophys. Res.*, 101, 90019015.

Eluszkiewicz, J., D. Crisp, R. W. Zurek, L. S. Elson, E. F. Fishbein, L. Froidevaux, J. W. Waters, R. Grainger, A. Lambert, R. S. Harwood, and G. E. Peckham, 1996: Residual circulation in the stratosphere and lower mesosphere as diagnosed from Microwave Limb Sounder data, *J. Atmos Sci.*, *53, 217-240.*

Fishbein, E. F., L. S. Elson, L. Froidevaux, G. L. Manney, W. G. Read, J. W. Waters, and R. W. Zurek, 1993: MLS observations of stratospheric waves in temperat ure and 0_3 during the 1992 southern winter, *Geophys. Res. Lett.*, '20, 1255 1258.

, R, E. Cofield, L. Froidevaux, R. F. Jarnot, T. A. Lungu, W. G. Read, Z. Shippony, J. W. Waters, I. S. McDermid, T. J. McGee, U. Singh, M. Gross, A. Hauchecorne, P. Keckhut, M. E. Gelman, and R. M. Nagatani, 1996: Validation of UARS Microwave Limb Sounder temperature and pressure measurements, *J. Geophys. Res.*, 101, 9938 10,016.

Froidevaux, L., J. W. Waters, W. G. Read, L. S. Elson, W. G. Read, D. A. Flower, and R. F. Jarnot, 1994: Global ozone observations from UARS MIS: an overview of zonal mean results, *Journal of Atmos Sci. (special issue on UARS early* scientific *results),* 51, 2846 2866.

, W. G. Read, T. A. Lungu, R. E. Cofield, E. F. Fishbein, D. A. Flower, R. F. Jarnot, B. P. Ridenoure, Z. Shippony, J. W, Waters, J. J. Margitan, I. S. McDermid, R. A. Stachnik, G. E. Peckham, G. Braathen, T. Deshler, J. Fishman, D. J. Hofmann, and S. J. Oltmans, 1996: Validation of UARS Microwave Limb Sounder ozone measurements, *J. Geophys. Res.,* 101, 10,017- 10,OGO.

Geller, M. A., Y. Chi, R. B. Rood, A. R. Douglass, D. J. Allen, M. Cerniglia, and J. W. Waters, 1993: 3-D transport-chemistry studies of the stratosphere using satellite data together with data assimilat ion, in *The Role of the Stratosphere in Global Change,* edited by M.-I,. Chanin. Springier-Verlag NATO ASI Series, Vol. 18, New York.

, V. Yudin, A. R. Douglass, J. W. Waters, L. S. Elson, A. E. Roche, and J. M. Russell, 1995: UARS PSC, $ClONO_2$, HCl, and C1O measurements in early winter: Additional verification of the paradigm for chlorine activation, *Geophys. Res. Lett., 22, 2937-2940.*

Hartmann, G. K., R. M. Bevilacqua, P. R. Schwartz, N. Kämpfer, K. F. Künzi, C. P. Aellig, A. Berg, W. Boogaerts, B. J. Connor, C. L. Croskey, M. Dachler, W. Degenhardt, H. D. Dicken, D. Goldizen, D. Kriebel, J. Langen, A. Loidl, J. J. Olivero, T. A. Pauls, S. E. Puliafito, M. 1,. Richards, C. Rudin, J. J. Tsou, W. B. Waltman, G. Umlauft, and R. Zwick, 1996: Measurements of 0_3, H_2O and ClO in the middle at mosphere using the millimeter-wave atmospheric sounder (MAS), *Geophys. Res. Lett.*, 23, 2313 2316.

Harwood, R. S., E. S. Carr, L. Froidevaux, R. F. Jarnot, W. A. Lahoz, C. L. Lau, G. E. Peckham, W. G. Read, P. D. Ricaud, R. A. Suttie, and J. W. Waters, 1993: Springtime stratospheric water vapour in the southern hemisphere as measured by MLS, *Geophys. Res. Lett.*, 20, 1235 1238.

Hofmann, D. J., 1996: Recovery of antarctic ozone hole, *Nature,* 384, 222 223.

Jackman, C. H., E. L. Fleming, S. Chandra, D. B. Considine, and J. E. Rosenfield, 1996: Past, present, and future modeled ozone trends with comparisons to observed trends, *J. Geophys. Res.*, 101, 28,753-28,767.

Jarnot, R. F., R. E. Cofield, J. W. Waters, G. E. Peckham, and D. A. Flower, 1996: Calibration of the Microwave Limb Sounder on the Upper At mosphere Research Satellite, *J. Geophys. Res.*, 101, 9957-9982.

Kumer, J. B., J. L. Mergenthaler, and A. E. Roche, 1993: CLAES CH_4, N_2O and CCl_2F_2 global data, *Geophys. Res. Lett.*, 20, 1'239--1242.

Lahoz, W. A., E. S. Carr, L. Froidevaux, R. S. Harwood, J. B. Kumer, J. L. Mergenthaler, G. E. Peckham, W. G. Read, P. D. Ricaud, A. E. Roche, and J. W. Waters, 1993: Northern hemisphere mid-st ratosphere vortex processes diagnosed from H_2O, N_2O and potential vorticity, *Geophys. Res. Lett.*, 23(20), 2671-2674.

, A. O'Neill, E. S. Carr, R. S. Harwood, I,. Froidevaux, W. G. Read, J. W. Waters, J. B. Kumer, J. I,. Mergenthaler, A. E. Roche, G. E. Peckham, and R. Swinbank, 1994: Three-dimensional evolution of water vapour distributions in the northern hemisphere as observed by MLS, *Journal of Atmos Sci. (special issue on UARS early scientific results), 51, 2914–2930.*

, M. R. Suttie, L. Froidevaux, R. S. Harwood, C. L. Lau, T. A. Lungu, G. E. Peckham, H. C. Pumphrey, W. G. Read, Z. Shippony, R. A. Suttie, J. W. Waters, G. E. Nedoluha, S. J. Oltmans, J. Russell III, and W. A. Traub, 1996a: Validation of UARS Microwave Limb Sounder 183 GHz H_2O measurements, *J. Geophys. Res.*, 101, 10,129 10,149.

, A. O'Neill, A. Heaps, V. D. Pope, R. Swinbank, R. S. Harwood, L. Froidevaux, W. G. Read, J. W. Waters, and G. E. Peckham, 1996b: Vortex dynamics and the evolution of water vapour in the stratosphere of the southern hemisphere, Q. *J. Roy. Met. Sot.*, **122, 423 450.**

Lau, C. L., G. E. Peckham, R. A. Suttic, and R. F. Jarnot, 1996: Characterisation of MLS I/f noise parameters, *Int. Jnl. Remote Sensing, 17, 3751-3759.*

Lefèvre, F., G. P. Brasseur, I. Folkins, A. K. Smith, and P. Simon, 1994: Chemistry of the 1991-92 stratospheric winter: Three-dimensional model simulations, *J. Geophys. Res.*, 99, 8183 8195.

Limpasuvan, V., and C. B. Leovy, 1995: Observations of the t wo-day wave near the southern summer stratopause, *Geophys. Res. Lett.*, 22, 2385-2388.

Lindzen, R. S., 1990: Sornc coolness concerning global warming, *Bull. Am. Meteorol. Soc., 71, 288 299.*

Lutrnan, E. R., J. A. Pyle, M. P. Chipperfield, D. J. Lary, , 1. Kilbane-Dawe, J. W. Waters, and N. Larsen, 1997: Three dimensional st udies of the 1 '391/92 Nort hern Hemisphere winter using domain-filling t rajectories with chemist ry, *J. Geophys. Res.*, 102, 14791488.

Mackenzie, I., R. S. Harwood, L. Froidevaux, W. G. Read, and J. W. Waters, 1996: Chemical loss of polar vortex ozone inferred from UARS MLS measurements of ClO during the Arctic and Antarctic springs of 1993, *J. Geophys. Res.*, 101, 14,505 14518.

Manney, G. I.., L. Froidevaux, J. W. Water's, L. S. Elson, E. F. Fishbein, R. W. Zurek, R. S. Harwood, and W. A.

Lahoz, 1993: The evolution of ozone observed by UARS MLS in the 1992 late winter southern polar vortex, *Geophys. Res. Lett.*, *20, 1279 1282.*

, - , - , R. W. Zurck, W. G. Read, L. S. Elson, J. B. Kumer, J. L. Mergenthaler, A. E. Roche, A. O'Neill, R. S. Harwood, I. MacKenzie, and R. Swinbank, 1994: Chemical depletion of ozone in the Arctic lower stratosphere during winter 1992-93, *Nature,* 370, 429 434.

, R. W. Zurek, L. Froidevaux, and J. W. Waters, 1995a: Evidence for arctic ozone depletion in late February and ' early March 1994, *Geophys. Res. Lett.*, 22, 2941-2944.

, L. Froidevaux, J. W. Waters, and R. W. Zurck, 1995b: Evolution of microwave limb sounder ozone and the polar vortex during winter, *J. Geophys. Res.,* 100, 2953 2972.

, L. Froidevaux, J. W. Waters, R. W. Zurek, J. C. Gille, J. B. Kurncr, J. L. Mergenthaler, A. E. Rochc, A. O'Neill, and R. Swinbank, 1995c: Formation of low ozone pockets in the middle stratosphere anticyclone during winter, *J. Geophys. Res.,* 100, 13,939 13,950.

, R. W. Zurek, W. A. Lahoz, R. S. Harwood, J. B. Kurncr, J. Mergenthaler, A. E. Roche, A. O'Neill, R. Swinbank, and J. W. Waters, 1995d: Lagrangian transport calculations using UARS data. Part I. : Passive tracers, *Journal of Atmos Sci.*, *52, 3049 3068.*

, R. W. Zurek, L. Froidevaux, J. W. Waters, A. O'Neill, and R. Swinbank, 1995e: Lagrangian transport calculations using UARS data. Part 11: Ozone, *Journal of Atmos Sci.*, *52, 3069 3081.*

, I,. Froidevaux, J. W. Waters, M. I.. Santee, W. G. Read, D. A. Flower, R. F. Jarnot, and R. W. Zurck, 1996a: Arctic ozone depletion observed by UARS MLS during the 1994 95 winter, *Geophys. Res. Lett.*, *23,* 85 *88.*

, M. L. Santee, I,. Froidevaux, J. W. Waters, and R. W. Zurek, 1996b: Polar vortex conditions during the 199596 arctic winter: Meteorology and MLS ozone, *Geophys. Res. Lett.*, *23, 3203-3206.*

, L. Froidevaux, M. L. Santee, R. W. Zurck, and J. W. Waters, 1997a: MLS observations of Arctic ozone loss in 1996-97, *Geophys. Res. Lett.*, in review.

, J. C. Bird, D. P. Donovan, T. J. Duck, J. A. Whiteway, S. R. Pal, and A. 1. Carswell, 1997b: Modelling ozone laminae in ground-based Arctic wintertime observations using trajectory calculations and satellite data, *J. Geophys.* Res., in review.

Massie, S. T., J. E. Dye, D. Baumgardner, W. J. Randel, F. Wu, X. X. Tie, L. Pan, F. Figarol, G. P. Brasseur, M. L. Santee, W. G. Read, R. G. Grainger, A. Lambert, J. I,. Mergenthaler, and A. Tabazadeh, 1997: Simultaneous observations of polar stratospheric clouds and HNO_3 over Scandinavia in January, 1992, *Geophys. Res. Lett.*, *24,* 595 598.

Morris, G. A., M. R. Schoeberl, L. Sparling, P. A. Newman, L. R. Lait, I,. S. Elson, J. W. Waters, A. E. Roche, J. B. Kumer, and J. M. Russell, 1995: Trajectory mapping of Upper Atmosphere Research Satellite (UARS) data, *J. Geophys. Res.,* 100, 16,491 16,505.

Mote, P. W., K. H. Rosenlof, J. R. Holton, R. S. Harwood, and J. W. Waters, 1995: Seasonal variation of water vapour in the tropical lower stratosphere, *Geophys. Res. Lett.*, 22, 1093 1096.

, K. H. Rosenlof, M. E. McIntyre, E. S. Carr, J. R. Holton, J. S. Kinnersley, H. C. Pumphrey, J. M. Russell III, J. W. Waters, and J. C. Gille, 1996: An atmospheric tape recorder: the imprint of tropical tropopause temperatures on stratospheric water vapor, *J. Geophys. Res.*, 101, 3989 4006.

Newell, R. E., Y. Zhu, E. V. Browell, S. Ismail, W. G. Read, J. W. Waters, K. K. Kelly, and S. C. Liu, 1996a: Upper tropospheric water vapor and cirrus: Comparison of DC-8 Observations, preliminary UARS microwave limb sounder measurements and meteorological analyses, *J. Geophys. Res.*, 101, 1931-1941.

, Y. Zhu, E. V. Browell, W. G. Read, and J. W. Waters, 1996b: Walker circulation and tropical upper tropospheric water vapor, *J. Geophys. Res.*, 101, 1961-1974.

- , Y. Zhu, W. G. Read, and J. W. Waters, Relationship between tropical upper t ropospheric moisture and eastern tropical Pacific sca surface temperat ure at seasonal and interannual t imc scales, 1997: *Geophys. Res. Lett.*, 24, 25 28.

Oh, J. J., and E. A. Cohen, 1992: Pressure broadening of ozone lines near 184 and 206 GHz by nit rogen and oxygen, *J. Quant. Spectrosc. Radiat. Transfer, 48, 405408.*

, and E. A. Cohen, 1994: Pressure broadening of ClO by N_2 and O_2 near 204 and 649 GHz and ncw frequency measurements bet wccn 632 and 725 GHz, *J. Quant. Spectrosc. Radiat. Transfer, 54, 151-156.*

Orsolini, Y. J., G. Hansen, U. Hoppe, G, I,. Manney, and K. Fricke, 1997: Dynamical modelling of wintertime lidar observations in the arctic: Ozone laminae and ozone depletion, Q. J. Roy. *Met. Sot.*, **123, 785 800.**

Pickering, K. E., A. M. Thompson, Y. Wang, W. Tao, D. P. McNamara, V. W. J. H. Kirchhoff, B. G. Heikes, G. W. Sachse, J. D. Bradshaw, G. L. Gregory, and D. R. Blake, 1996: Convect ive transport of biomass burning emissions over Brazil during TRACE A, *J. Geophys. Res.*, 101, 23,993 24,012.

Pickett, H. M., D. E. Brims, and E. A. Cohen, 1981: Pressure broadening of C1O by nitrogen, *J. Geophys. Res.*, 86, 7279 7282.

, R. L. Poyntcr, and E. A. Cohen, 1992: Submillimeter, millimeter and microwave spectral line catalog,.Tech. Rep. 80-23, rev. 3, Jet Prop. Lab., Pasadena, Calif.

Pumphrey, H. C., 1997: Nonlinear retrievals of water vapour from the UARS Microwave Limb Sounder (MLS), *Adv. Space. Res.* in press.

and R. S. Harwood, 1997: Water vapour and ozone in the mesosphere as measured by UARS MLS, *Geophys. Res. Lett. 24, 1399 2002.*

Randel, W. J., J. C. Gille, A. E. Roche, J. B. Kumer, J. L. Mergenthaler, J. W. Waters, E. F. Fishbein, and W. A. Lahoz, 1993: Stratospheric transport from the tropics to middle latitudes by plauctary-wave mixing, *Nature, 365,* 533 535.

, G. L. Manney, W. G. Read, L. Froidevaux, and J. W. Waters, 1996b: Polar vortex conditions during the 1995 96 arctic winter: MLS C1O and HNO_3, *Geophys. Res. Lett.*, *23, 3207-3210.*

, , L. Froidevaux, R. W. Zurek, and J. W. Waters, 1997a: MLS observations of C1O and HNO_3 in the 1996-97 Arctic polar vortex, *Geophys. Res. Lett.*, in review.

, A. Tabazedeh, G. L. Manney, R. J. Salawitch, L. Froidevaux, W. G. Read, and J. W. Waters, 1997b: UARS MLS HNO_3 observations: Implications for Antarctic PSCs, *J. Geophys. Res.*, in review,

Schoeberl, M. R., R. S. Stolarski, A. R. **Douglass**, P. A. Newman, L. R. Lait, J. W. Waters, L. Froidevaux, and W. G. Read, 1993: MLS ClO observations and arctic polar vortex temperatures, *Geophys. Res. Lett.*, *20, 2861-2864.*

, A. R. Douglass, S. R. Kawa, A. E. Dessler, P. A. Newman, R. S. Stolarski, A. E. Roche, L. Froidevaux, J. W. Waters, and J. M. Russell 111, 1996: 'The development of the Antarctic ozone hole, *J. Geophys. Res.*, 101, 20,909 20,924.

, A. E. Roche, J. M. Russell III, D. Ortland, P. B. Hays, and J. W. Waters, 1997: An estimation of the dynamical isolation of the tropical lower stratosphere using UARS wind and trace gas observations of the quasi-biennial oscillation, *Geophys. Res. Lett.*, *24, 53-56.*

Siegel, P. H., I. Mchdi, R. J. Dengler, J. E. Oswald, A. Pease, T. W. Crowe, W. Bishop, Y. Li, R. J. Mattauch, S. Weinreb, J. East, and T. Lee, 1993: Heterodyne radiometer development for the Earth Observing System Microwave Limb Sounder, in *Infrared and Millimeter- Wave Engineering, SPIE vol. 1874*, pp. 124-137.

Singh, U. N., P. Keckhut, T. J. McGee, M. R. Gross, A. Hauchecorne, E. F. Fishbein, J. W. Waters, J. C. Gille, A. E. Roche, and J. M. Russel, *1996:* Stratospheric temperature measurements by two collocated NDSC lidar during UARS validation campaign, *J. Geophys. Res.*, 101, 10,287-10,297.

Solomon, s., and R. R. Garcia, 1984: On the distributions of long-lived tracers and chlorine species in the middle atmosphere, *J. Geophys. Res., 89,* 11,633-11,644.

, S. Borrmann, R. R. Garcia, R. Portmann, L. Thomason, L. R. Poole, D. Winker, and M. P. McCormick, 1997: Heterogeneous chlorine chemistry in the tropopausc region, *J. Geophys. Res.* in press.

Stachnik, R. A., J. C. Hardy, J. A. Tarsala, J. W. Waters, and N. R. Erickson, 1992: Submillimeterwave heterodyne measurements of stratospheric C1O, HCl, 0_3, and 110_2: First results, *Geophys. Res. Lett.*, **19**, 1931-1934,

Stone, E. M., J. L. Stanford, J. R. Ziemke, D. R. Allen, F. W. Taylor, C. D. Rodgers, B. N. Lawrence, E. F. Fishbein, L. S. Elson, and J. W. Waters, 1995: Space-time integrity of improved stratospheric and mesospheric sounder and microwave limb sounder temperature fields at Kelvin wave scales, *J. Geophys. Res.*, 100, *14,089-14,096.*

, W. J. Randel, J. L. Stanford, W. G. Read, and J. W. Waters, 1996: Baroclinic wave variations observed in MLS upper tropospheric water vapor, *Geophys. Res. Lett.*, *23,* 2967 *2970.*

Tabazadeh, A., R. P. Turco, K. Drdla, M. Z. Jacobsen, and O. B. Toon, 1994: A study of type I polar stratospheric cloud formation, *Geophys. Res. Lett.*, **21**, 1619 **1622.**

, F. Wu, J. M. Russell 111, J. W. Waters, and 1,. Froidevaux, 1995: Ozone aud temperature changes in the stratosphere following the eruption of Mount Pinatubo, *J. Geophys. Res.*, **100,** 16,753 *16,754.*

Ray, E., J. R. Holton, E. F. Fishbein, L. Froidevaux, and J. W. Waters, 1994: The tropical semiannual oscillation in temperature and ozone observed by the MLS, *Journal of Atmos Sci. (special issue on UARS early scientific results), 51,* 3045 3052.

Read, W. G., L. Froidevaux, and J. W. Waters, 1993: Microwave Limb Sounder (MLS) measurements of SO_2 from Mt. Pinatubo volcano, *Geophys. Res. Lett., 20, 1299 1302.*

, J. W. Waters, L. Froidevaux, D. A. Flower, R. F. Jarnot, D. L. Hartmann, R. S. Harwood, and R. B. Rood, 1995: Upper-tropospheric water vapor from UARS MLS, *Bull. Am. Meteorol. Sot., 76, 2381-2389.*

Reber, C. A., 1993: The Upper At mosphere Research Satellite (UARS), *Geophys. Res. Lett., 20,* 1215 *1218.*

- , *C.* E. Trevathan, R. J. McNeal, and M. R. Luther, 1993: The Upper Atmosphere Research Satellite (UARS) mission, *J. Geophys. Res., 98, 10,643--10,647.*

Redaelli, G., L. Lait, M. Schoeberl, P. A. Newman, G. Visconti, A. D'Altorio, F. Masci, V. Rizi, L. Froidevaux, J. Waters, and J. Miller, 1994: UARS MLS 0_3 soundings compared with lidar measurements using the conservative coordinates reconstruction technique, *Geophys. Res. Lett.,* 21, 1535 1538.

Reichardt, J., A. Ansrnann, M. Screazi, C. Weit kamp, and W. Michaelis, 1996: Unexpectedly low ozone concentration in midlatitude t roposphcric icc clouds: a case study, *Geophys. Res. Lett.*, 23, 1929 1932.

Ricaud, P., J. dc La Noë, B. J. Connor, L. Froidevaux, J. W. Waters, R. S. Harwood, I. A. MacKenzie, and G. E. Peckham, 1996: Diurnal variability of mesospheric ozone as measured by the UARS microwave limb sounder iustrurncnt: Theoretical and ground-based validations, *J. Geophys. Res.*, 101, 10,077-10,089.

, E. S. Carr, R. S. Harwood, W. A. Lahoz, L. Froidevaux, W. G. Read, J. W. Waters, J. L. Mergenthaler, J. B. Kumcr, A. E. Rochc, and G. E. Peckham, 1995: Polar stratospheric clouds as deduced from MLS and CLAES measurements, *Geophys. Res. Lett., 22, 2033* 2036.

Roscoe, H.K, A.E. Jones, A.M. Lee, 1997: Midwinter start to Antarctic ozone depletion: evidence from observations and models, Science, in press.

Rosenlof, K. H., 1995: Seasonal cycle of the residual mean meridional circulation in the st ratosphere, *J. Geophys. Res.*, 100, 5173 5191.

Santcc, M. L., W. G. Read, J. W. Waters, L. Froidevaux, G. I,. Manney, D. A. Flower, R. F. Jarnot, R. S. Harwood, and G. E. Peckham, 1995: Interhemispheric differences in polar stratospheric HNO_3, H_2O, C1O and 0_3, Science, 267, 849 852.

, L. Froidevaux, G. L. Manney, W. G. Read, J. W. Waters, M. P. Chipperfield, A. E. Roche, J. B. Kumer, J. I,. Mergenthaler, and J M Russell III, 1996a: Chlorine deactivation in the lower stratospheric polar regions during late winter: Results from UARS, *J. Geophys. Res.*, 101, 18,835 18,859.

Thompson, A. M., K. E. Pickering, I). P. McNamara, M. R. Schoeberl, R. D. Hudson, J. H. Kim, E. V. Browell, V. W. J. H. Kirchhoff, and D. Nganga, 1996: Where did tropospheric ozone over southern Africa and the tropical Atlantic come from in October 1992? Insights from TOMS, GTE TRACE A, and SAFARI 1992, *J. Geophys. Res.*, 101, 24,251 24,278.

Toumi, R., and S. Bekki, 1993: The importance of t he react ions between OH and C1O for stratospheric ozone, *Geophys. Res. Lett.*, *20, 2447-2450.*

Waters, J. W., 1989: Microwave limb-sounding of Earth's upper atmosphere, *Atmos. Res.*, *23,* 391-410.

, 1992a: Submillimeter heterodyne spectroscopy and remote sensing of the upper atmosphere, *IEEE Proc.*, *80, 1679 1701.*

, 1992b: Submillimeter Hctcrodync Spect roscopy and Remote Sensing of t he Upper Atmosphere, in *The use of EOS for Studies of Atmospheric Physics,* edited by J. C. Gille, and G. Visconti, pp. 491-579. North Holland Elsevier, Amsterdam.

, 1993: Microwave Limb Sounding, in *Atmospheric Remote Sensing by Microwave Radiometry,* edited by M. A. Janssen, chap. 8. John Wiley, Ncw York.

, 1997a: Atmospheric measurements by the MLS experiments: Results from UARS and plans for the future, *Adv. Space Res.* in press.

, 1997b: The Upper Atmosphere Research Satellite (UARS), in *The Stratosphere and Its Role in the Climate* System, edited by G. P. Brasseur. Springler-Verlag NATO ASI Series, Ncw York, in press.

, J. J. Gustincic, R. K. Kakar, H. K. Roscoe, P. N. Swanson, T. G. Phillips, T. DeGraauw, A. R. Kerr, and R. J. Mat tauch, 1979: Aircraft search for millimeter wavelength emission by st ratospheric C1O, *J. Geophys. Res., 84,* 6934.

, - , *P. N.* Swanson, and A. R. Kerr, 1980: Measurements of upper at mospheric H_2O emission at 183 GHz, in *A tmospheric Water Vapor,* edited by Wilkerson, and Ruhnke, pp. 229 240. Academic Press, New York.

-, J. C. Hardy, R. F. Jarnot, and H. M. Pickett, 1981: Chlorine monoxide radical, ozone, and hydrogen peroxide: Stratospheric measurements by microwave limb sounding, Science, 214, 61-64.

, - , - , , and P. Zimmermann, 1984: A balloon-borne microwave limb sounder for stratospheric measurements, *J. Quant. Spectrosc. Radiat. Transfer, 32, 407-433.*

) R. A. Stachnik, J. C. Hardy, and R. F. Jarnot, 1988: ClO and 0_3 stratospheric profiles: Balloon microwave measurements, *Geophys. Res. Lett.*, *15, 780-783.*

, I,. Froidevaux, G. L. Manney, W. G. Read, and L. S. Elson, 1993a: Lower stratospheric C1O and 0_3 in the 1992 southern hemisphere winter, *Geophys. Res. Lett.*, *20,* 1219 1222.

, , W. G. Read, G. L. Manney, L. S, Elson, I). A. Flower, R. F. Jarnot, and R. S. Harwood, 1993b: Stratospheric ClO and ozone from the Microwave Limb Sounder on the Upper Atmosphere Research Satellite, Nature, 362,

597 *602.*

, G.L. Manney, W. G. Read, L. Froidevaux, D. A. Flower, and R. F. Jarnot, 1995: UARS MLS observations of lower stratospheric C1O in the 1992-93 and 199394 arctic winter vortices, *Geophys. Res. Lett.*, *22, 823826.*

, W. G. Read, L. Froidevaux, T. A. Lungu, V. S. Perun, R. A. Stachnik, R. F. Jarnot, R. E. Cofield, E. F. Fishbein, D. A. Flower, J. R. Burke, J. C. Hardy, L. L. Nakamura, B. P. Ridenoure, Z. Shippony, R. P. Thurstans, L. M. Avallone, D. W. Toohcy, R. L. dcZafra, and D. T. Shindell, 1996: Validation of UARS Microwave Limb Sounder C1O measurements, *J. Geophys. Res.*, **101, 10,091-10,127,**

Wcinrcb, S., 1997: Millimeter- Wave Integrated-Circuit Radiometers, in Passive hlillinlctcr-Wave Technology, Roger M. Smith, editor, *SPIE Proceedings, 3064, 8089.*

, P.C. Chao, W. Copp, 1997: Full Waveguide Band, 90 to 140 GHz MMIC Amplifier Module, 1997 *IEEE MTT-S Digest, 1279-1280.*

Wild, J. D., M. E. Gelman, A. J. Miller, M. L. Chanin, A. Hauchecorne, P. Keckhut, R. Farley, P. D. Dao, J. W. Mcriwethcr, G. P. Gobbi, F. Congeduti, A. Adriani, I. S. McDermid, 'I'. J. McGee, and E. F. Fishbein, 1995: Comparison of stratospheric temperature from several lidars, using National Meteorological Center and Microwave Limb Sounder data as transfer references, *J. Geophys. Res.*, **100, 11,105** 11,111.

Wu, D. L., and J. W. Waters, 1996a: Gravity-wave-scale temperat urc fluct uations seen by the UARS MLS, *Geophys. Res. Lett.*, *23, 3289 3292.*

, and - , 1996b: Satellite observations of atmospheric variances: a possible indication of gravity waves, *Geophys.* Res. *Lett.*, **23, 3631-3634.**

, and , 1997: Observations of gravity waves with t hc UARS Microwave Limb Sounder, in *Gravity Wave Processes and Their Parameterization in Global Climate Models,* edited by K. Hamilton, vol. 50, pp. 103 120. Springler-Verlag NATO ASI Series, Ncw York.

- -, E. F. Fishbein, W. G. Read, and J, W. Waters, 1996: Excitation and evolut ion of the quasi 2-day wave observed in UARS/MLS temperat urc measurements, *J. Atmos. Sci.*, 53, 728 738.

Ziemke, J. R., S. Chandra, A. M. Thompson, and D. P. McNamara, 1996: Zonal asymmetries in southern hemisphere column ozone: Implications of biomass burning, *J. Geophys. Res.*, **101, 14,421- 14,427.**

Formatted August 27, 1997 with AGU LaTeX macros v3.0, as modified by J. Waters in `jwwgrlpp.sty`. Input file: `JAS97REF`.

FIGURE CAPTIONS

Figure 1. Signal Flow Block Diagram of the Upper Atmosphere Research Satellite (UARS) Microwave Limb , Sounder (MLS).

Figure 2. ClO atmospheric thermal emission measured by UARS MLS and calculated from retrieved ClO vertical profiles (from Waters et al., 1996). The right panels are for lower stratospheric ClO, where the tangent point of the MLS field-of-view was between 22 and 100 hPa tangent pressure, and the measured spectrum is the average of data from 16 daytime limb scans made in the Antarctic vortex on 16 August 1992. The left panels are for upper stratospheric ClO, where the tangent point of the MLS field-of-view was between 2.2 and 10 hPa tangent pressure, and the measured spectrum is the average of 548 daytime limb scans made between 34 S and 80 N latitudes on 11 July 1993. The middle panels are the average of spectra calculated from individual ClO retrievals from these limb scans, and the bottom panels are the difference between measured and calculated. The horizontal bars indicate the spectral resolution of individual filters (all of which are sampled simultaneously) and the vertical bars indicate the expected noise in the average.

Figure 3. MLS 205 GHz radiances (wing channel of ClO band) from the lower stratosphere (50 hPa tangent pressure) versus latitude on21 September 1991. The tropical lower stratosphere had very heavy loading of aerosol from the Pinatubo volcano at this time, but the MLS radiances are not attenuated by this aerosol layer, as expected, with an observational upper limit of-O. 10/0 opacity through the limb path at 205 GHz.

Figure 4. Results of comparing MLS ozone with other well-calibrated near-coincident measurements (adapted from Froidevaux et al., 1996, and Cunnold et al., 1996a). Points A are the average differences of SAGE II measurements selected in low aerosol situations, covering 25 N to 55 N latitudes, and made between September 1991 and December 1993. Points T are average differences of 295 Table Mountain (34 N), California, profiles. Points B are average differences of 42 Boulder (40 N) ozonesondes. Points U are average differences of 8 balloon-borne ultraviolet photometer profiles, and Points S are average differences of 5 submillimeter limb sounder profiles.

Figure 5. Measurements obtained from UARS MLS. Dotted lines indicate zonal (or other) means, and the dashed line for ClO at lower altitudes indicates individual measurements when ClO is enhanced in the polar winter vortices.

Figure 6. ClO and ozone in the lower stratosphere through the Antarctic winter of 1992 (adapted from Waters et al., 1993 b). The daily maps shown here are for MLS profiles interpolated to 465 K potential temperature (around 18 km altitude in the polar vortex). Irregular white contours are potential vorticity values (-2.5 and -3.0×10^{-5} K $m^2 kg^{-1} s^{-1}$, calculated from the U.S. National Center for Environmental Predition operational data) which indicate the approximate edge of the dynamical vortex, and the thin white contour concentric with the pole on the C1O maps is the edge of polar night. The black contour of the ClO maps indicates the edge of daylight for the measurements, and thin green contours indicates temperatures of 190 and 195K.

Figure 7. MLS maps on the 465 K potential temperature surface for the earliest day each year which MLS observed enhanced ClO in the Antarctic vortex. White contours are potential vorticity as in Figure 6. The dashed curve is the edge of daylight for the measurements, and the solid black curves are temperatures of 195 and (when they exist) 188 K. These are not necessarily the earliest day each year Antarctic ClO was enhanced, just the earliest at which it was observed by MLS. Only in 1993 did MLS observations occur through the period of initial enhancement of Antarctic ClO; due to the UARS yaw state, or to operational constraints, observations in other years did not cover the period of transition to enhanced C1O. Slight differences from the 2 June 1992 ClO map in Figure 6 are because MLS Version 3 data are used in Figure 6 whereas Version 4 data are used here.

Figure 8. MLS maps of lower stratospheric ClO on 11 January 1992 (adapted from Waters et al., 1993a). This map is for data interpolated to 465K potential temperature. The white contour is potential vorticity (2.75x1 O-s K $m^2 kg^{-1}$ S-l contour) which indicates the approximate edge of the Arctic vortex, and the green contour is 195 K temperature (the nominal threshold for type-I PSC formation). The black contour indicates the edge of daylight for measurements. The color bar indicates ClO mixing ratios in parts per billion by volume.

Figure 9. MLS maps of lower stratospheric C1O and $HN0_3$, illustrating differences between the Arctic and Antarctic (adapted from Santee et al., 199S). The data are interpolated to 465 K potential temperature, white irregular contours are of potential vorticity (2.5 and 3.0x 105 K m^2 kg-' s-' contours) which indicate the approximate edge of the polar vortices, the thin white contour concentric with the south pole is the edge of polar night. Green contours indicate temperatures of 195 and 188 K.

Figure 10. MLS maps of lower stratospheric C1O in the Arctic vortex on 20 February of 1996 and 1997 (adapted from Santee et al., 1996b and 1997a). These maps are for the 465 K potential temperature surface; white contours are potential vorticity as in Figure 9 which indicate the approximate edge of the polar vortex and black contours indicate temperatures of 195 and 188 K.

Figure 11. MLS maps of water vapor and ozone at 655 K potential temperature (-25 km) on 4 and 5 November 1991 (adapted from Harwood et al., 1993).

Figure 12. Zonal mean daytime ClO from MLS for January-March 1993 (top) and July-September 1993 (bottom). The color bar is in parts per billion.

Figure 13. C1O trends observed by MLS at 2 hPa (top) and 22 hPa (bottom). These data (crosses) are zonal averages for 30S to 30N latitudes and the slanted straight lines are fits to the data (adapted from L. Froidevaux et al., manuscript in preparation).

Figure 14. Tropical Pacific upper tropospheric water vapor anomalies observed by MLS. These data show deviations from the mean of the preliminary retrievalsof215 hPa water vapor from UARS MLS. Notation along the left axis indicates whether or not an El Nino event occurred that year.

Figure 15. Some initial retrievals of cloud ice content from UARS MLS data (adapted from D. L. Wu et al., manuscript in preparation). The units are average density of the total ice content within the MLS observation volume, -3 km (vertical) x -300 km (horizontal along the line of sight) x ~30 km (horizontal orthogonal to the line of sight).

Figure 16. Signal flow diagram for the Earth Observing System Microwave Limb Sounder (EOS MLS) now under development.

Figure 17. EOS MLS spectral bands. The EOS MLS radiometers, except that operating near 118 GHz, are double-sideband (having approximately equal responses from intermediate frequencies, IFs, above and below the local oscillator, LO, frequency). The spectral bands in the IF frequencies of these radiometers are shown here, and each band contains a multifrequency filter bank spectrometer. The primary targeted molecules is indicated for each band, and a minus sign indicates the spectral line appears in the lower sideband of the radiometer. Asterixes indicate locations of additional individual filters, and bullets indicate locations of spectrometers with **high spectral resolution** for mesospheric signals. Numbers inside boxes indicate the IF frequencies of spectrometers which are centered on spectral lines of target molecules, and include the effects of orbital motion Doppler shifts.

Figure 18. EOS MLS measurements. Dotted lines indicate zonal (or other) means. Dashed lines indicate volcanic SO_2 and enhanced ClO. Hearts indicate measurement goals.

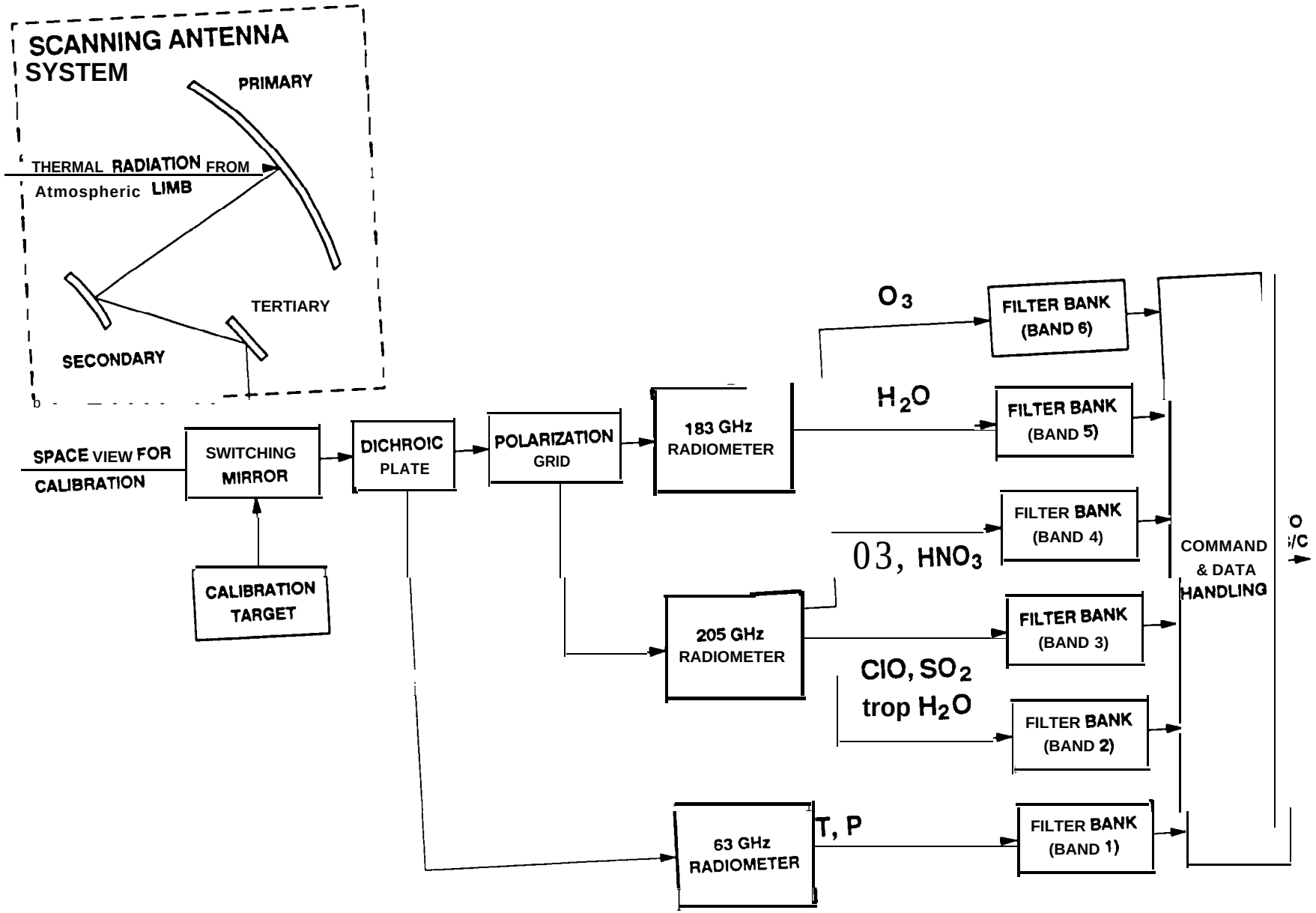
SCANNING ANTENNA SYSTEM
PRIMARY
THERMAL RADIATION FROM Atmospheric LIMB
TERTIARY
SECONDARY
SPACE VIEW FOR CALIBRATION
SWITCHING MIRROR
CALIBRATION TARGET
DICHROIC PLATE
POLARIZATION GRID
183 GHz RADIOMETER
205 GHz RADIOMETER
63 GHz RADIOMETER
O3
H2O
03, HNO3
ClO, SO2 trop H2O
T, P
FILTER BANK (BAND 6)
FILTER BANK (BAND 5)
FILTER BANK (BAND 4)
FILTER BANK (BAND 3)
FILTER BANK (BAND 2)
FILTER BANK (BAND 1)
COMMAND & DATA HANDLING

Figure 1

lower stratosphere

upper stratosphere

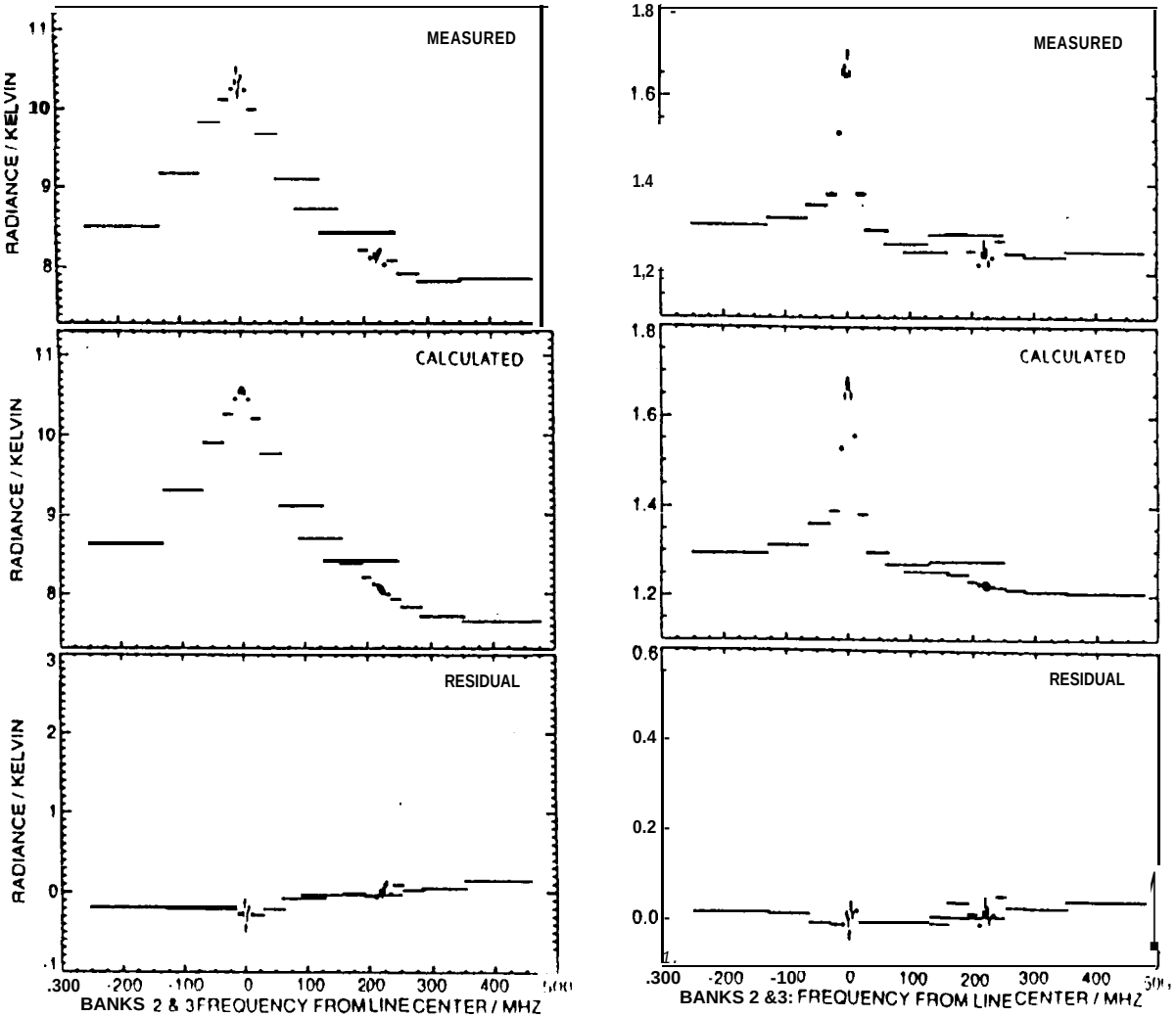

Figure 2

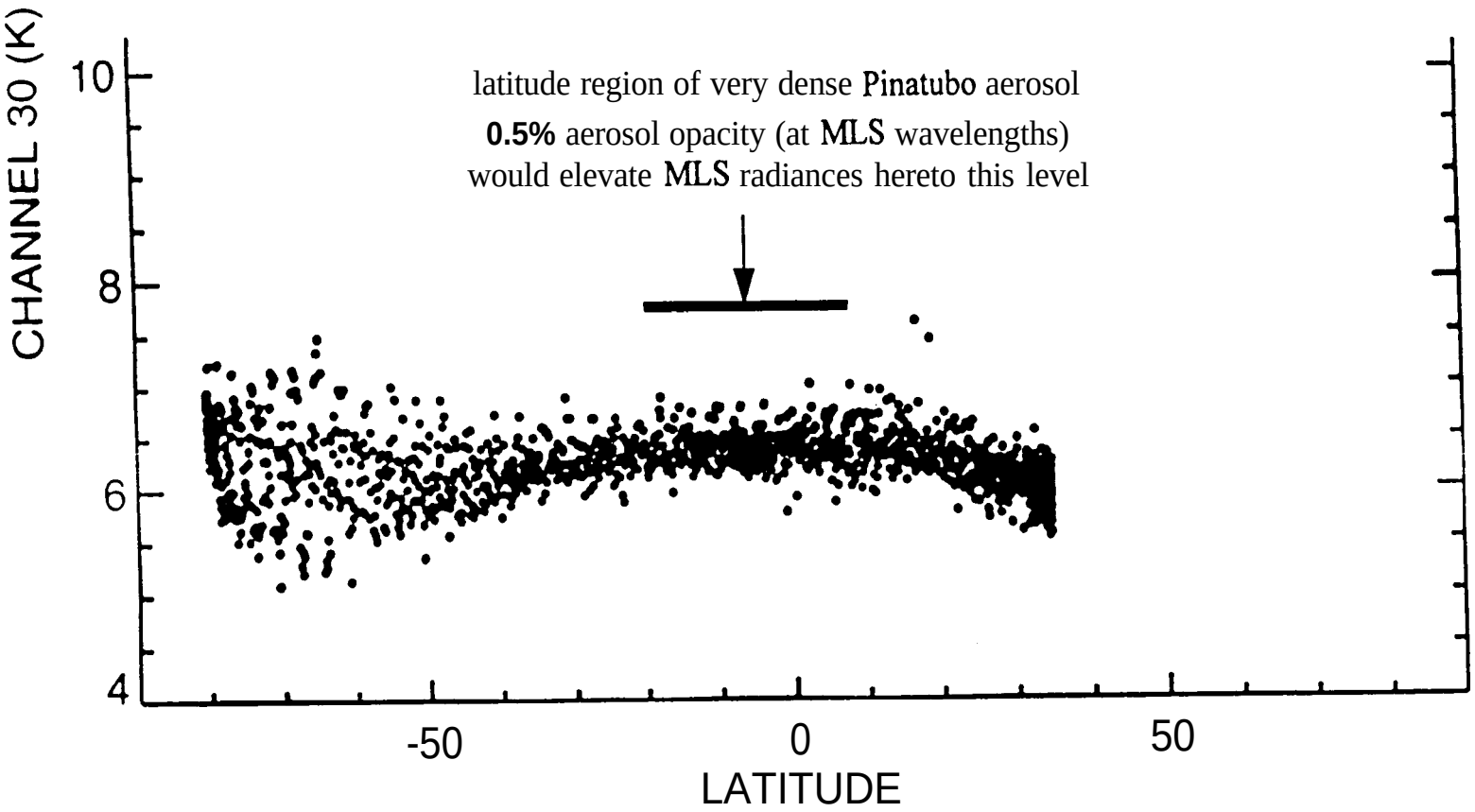
latitude region of very dense Pinatubo aerosol
0.5% aerosol opacity (at MLS wavelengths)
would elevate MLS radiances hereto this level
CHANNEL 30 (K)
10
8
6
4
-50
0
50
LATITUDE

Figure 3

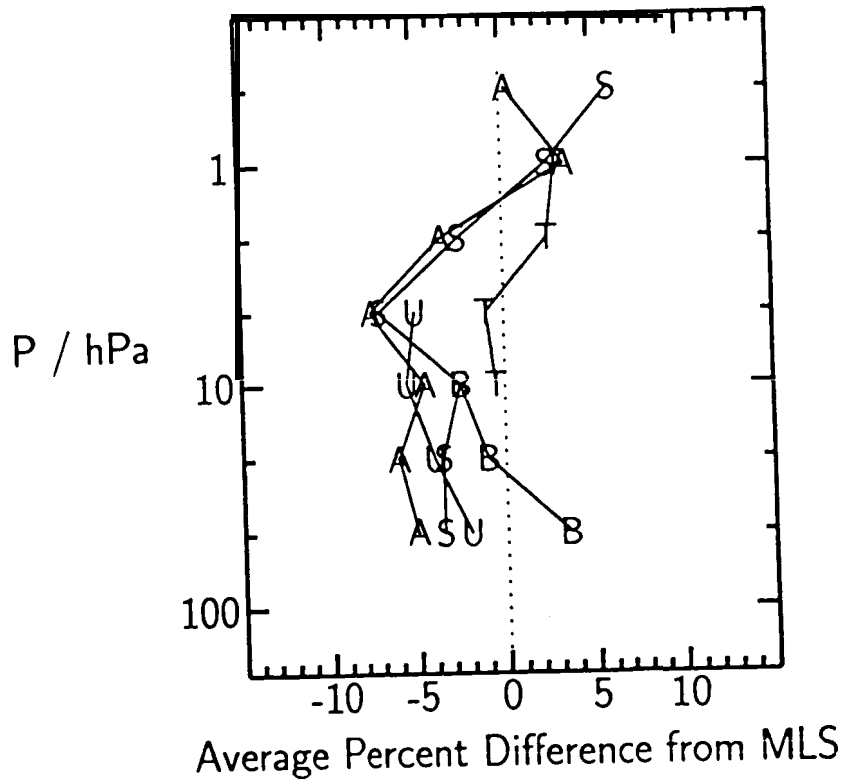

Figure 4

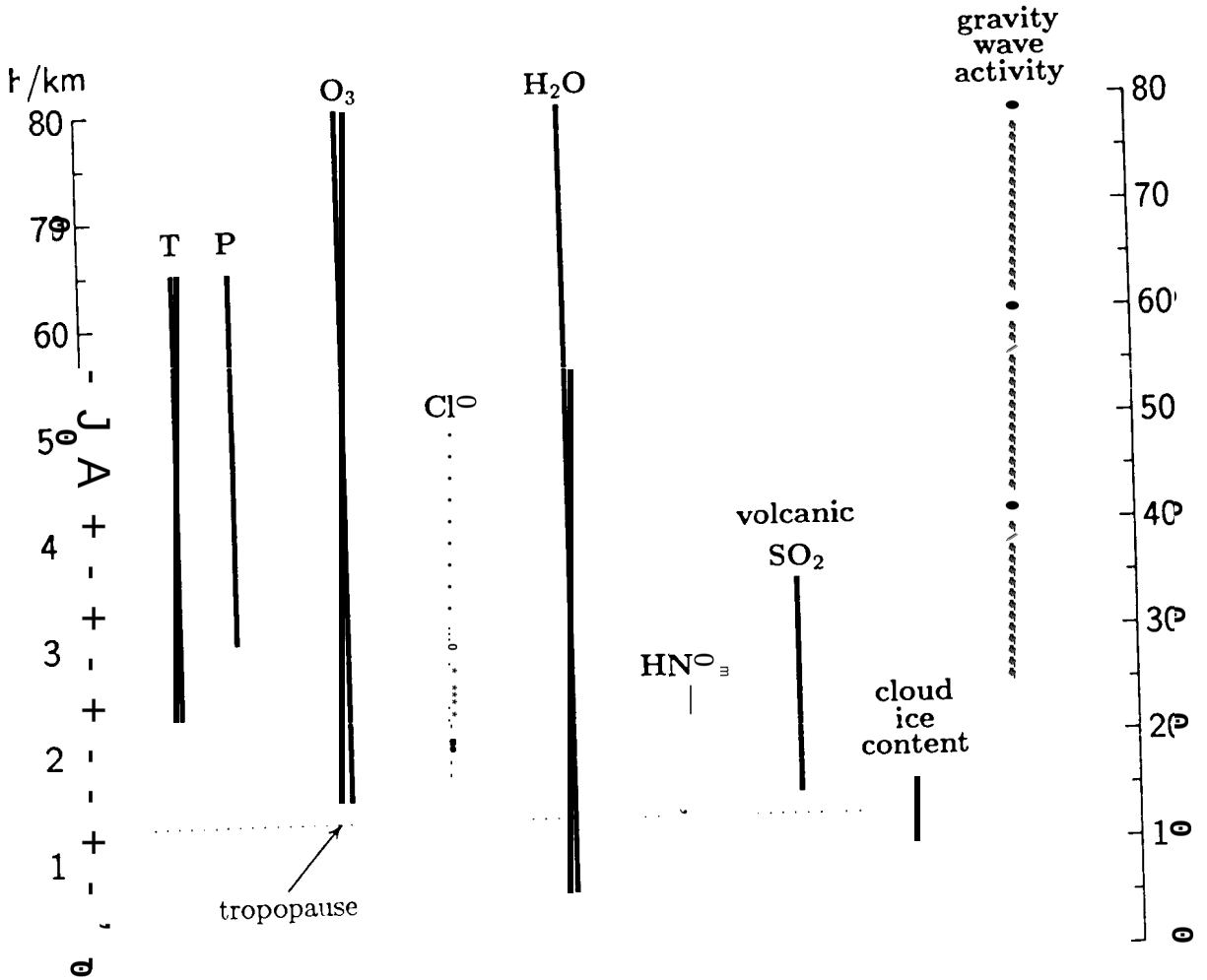
h/km
80
70
60
50
40
30
20
10
0
T
P
O_3
ClO
H_2O
HNO_3
volcanic
SO_2
cloud
ice
content
gravity
wave
activity
tropopause

Figure 5

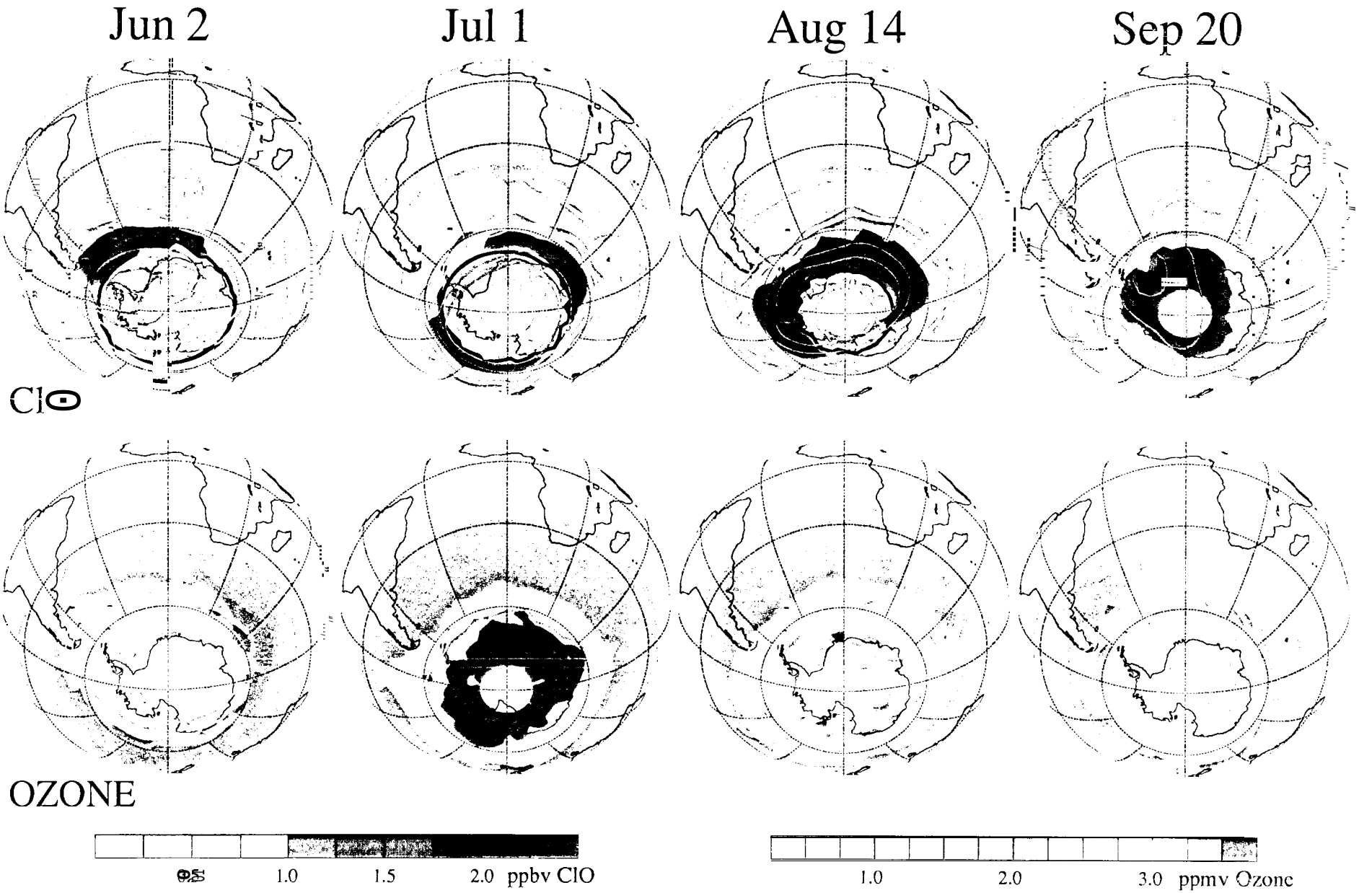
Jun 2
Jul 1
Aug 14
Sep 20
ClO
OZONE
0.5
1.0
1.5
2.0 ppbv ClO
1.0
2.0
3.0 ppmv Ozone

Figure 6

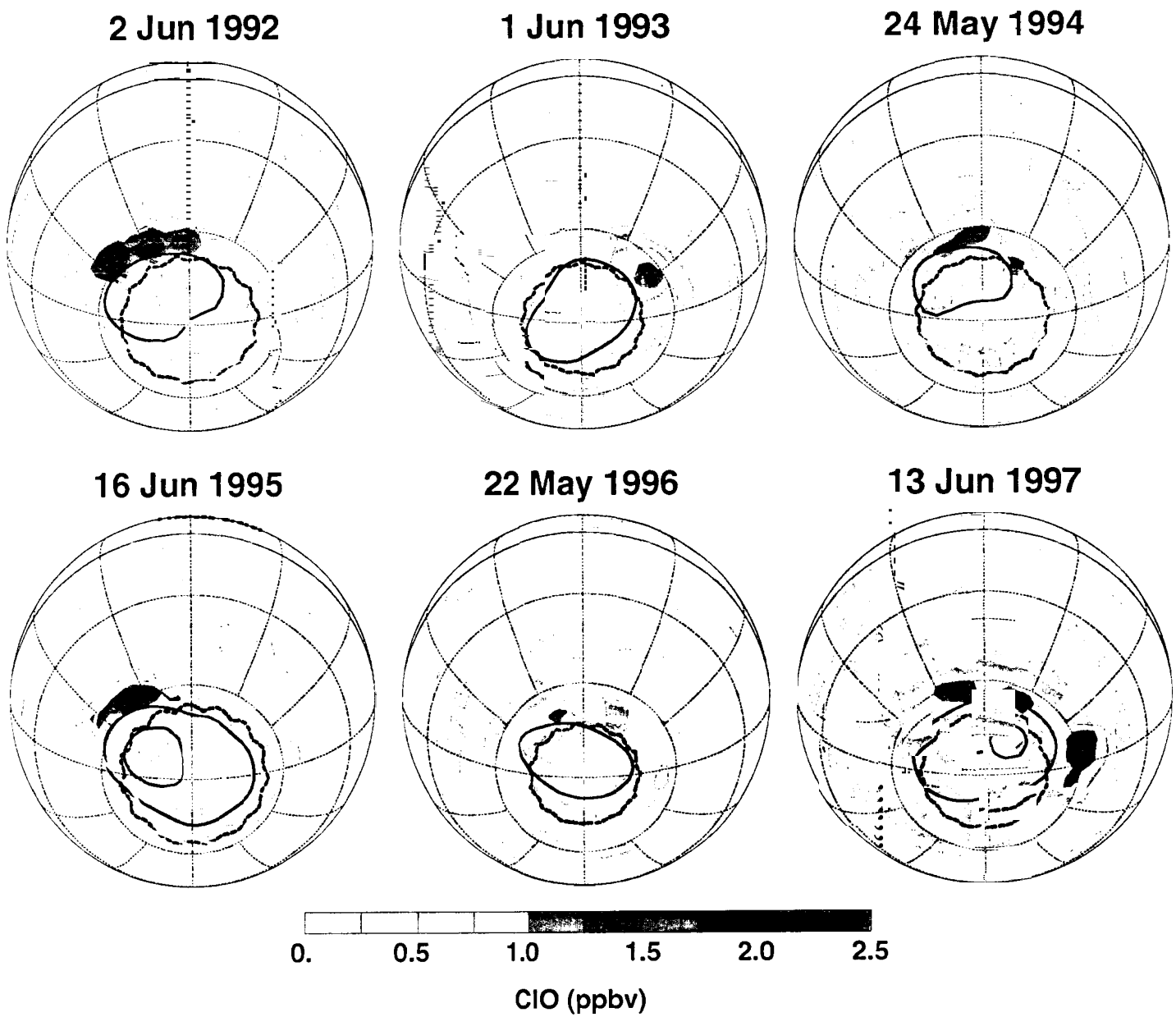
2 Jun 1992
1 Jun 1993
24 May 1994
16 Jun 1995
22 May 1996
13 Jun 1997
0.
0.5
1.0
1.5
2.0
2.5
ClO (ppbv)

Figure 7

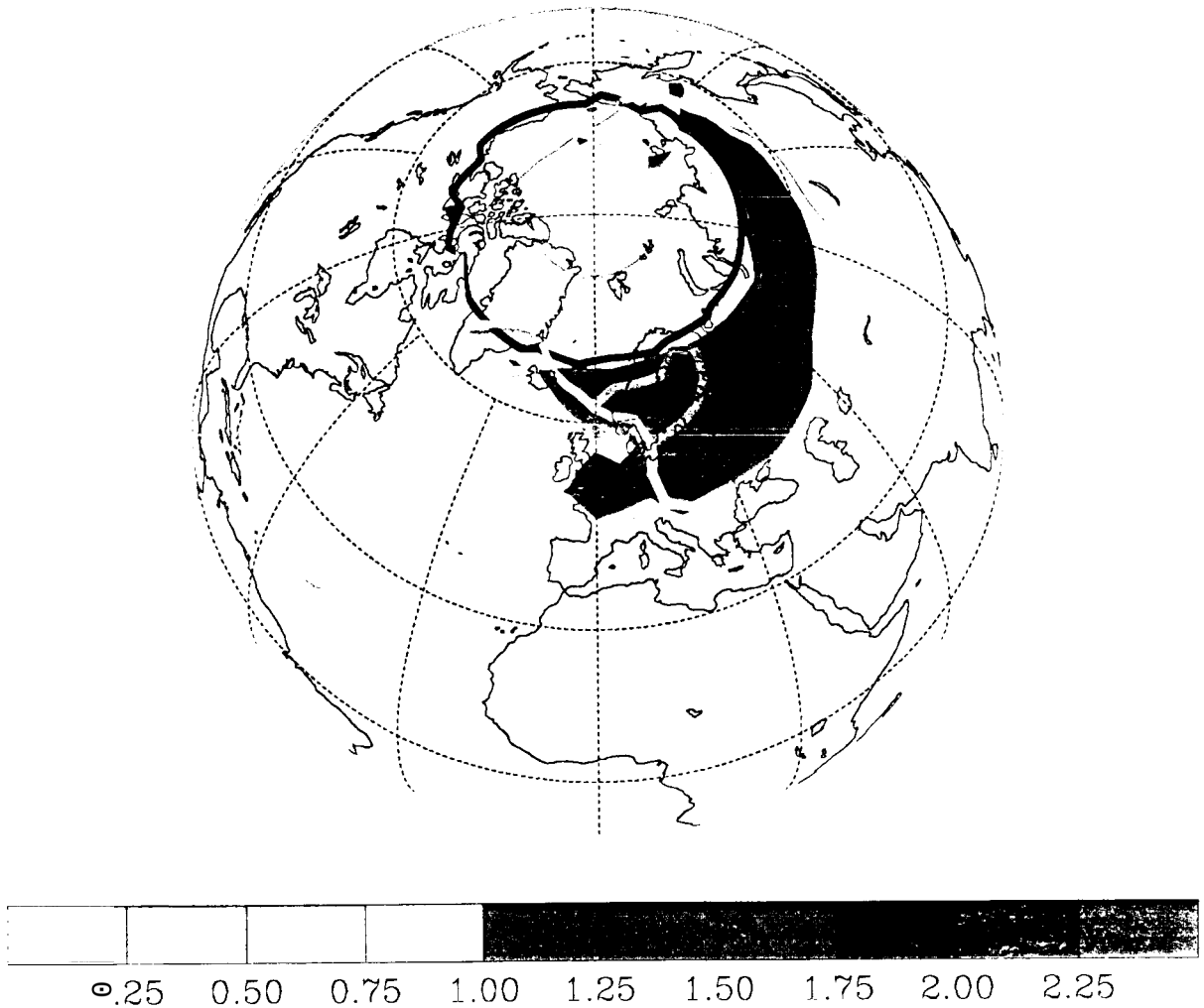

Figure 8

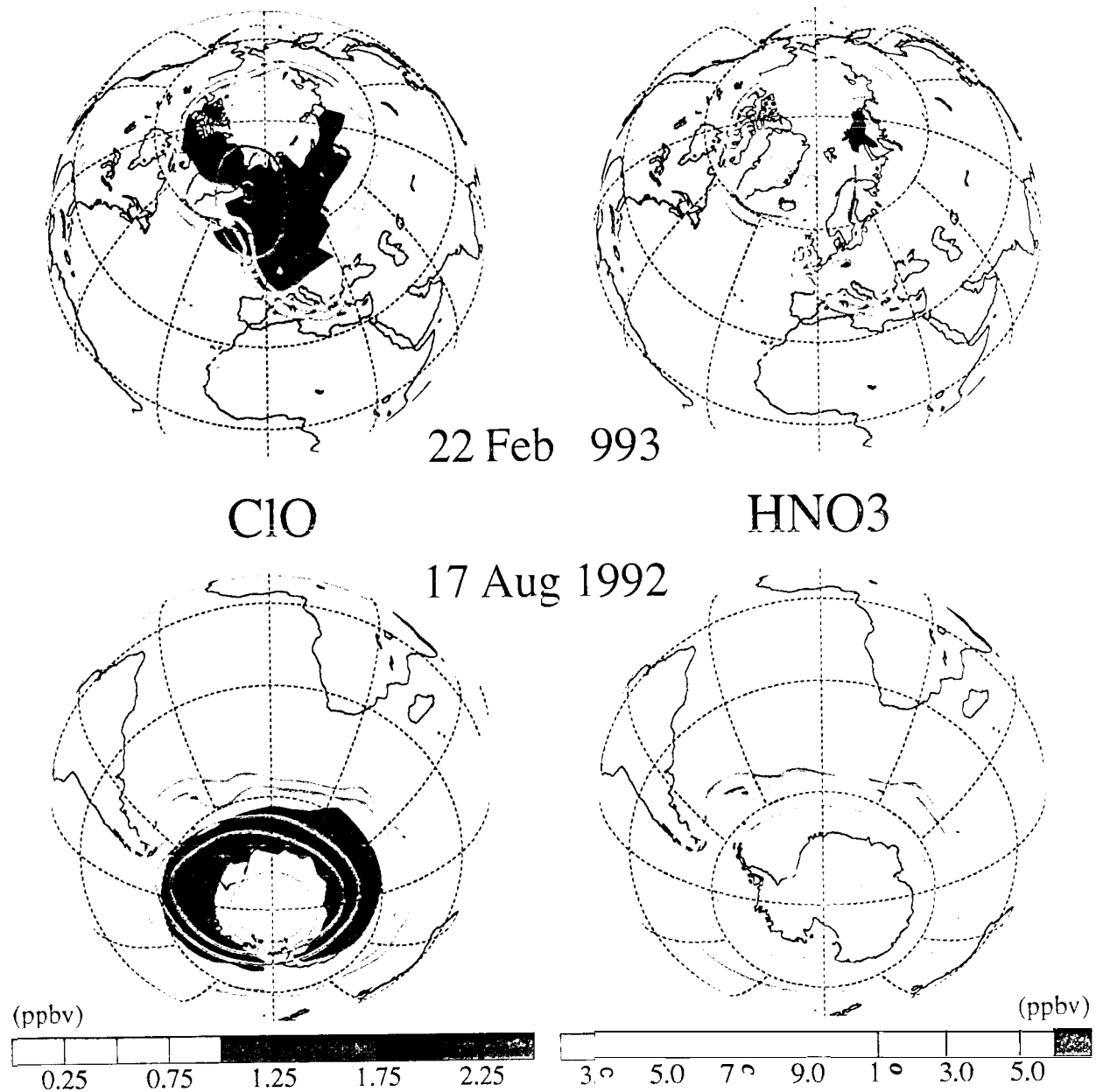
22 Feb 993
ClO
HNO3
17 Aug 1992
(ppbv)
0.25
0.75
1.25
1.75
2.25
(ppbv)
3.0
5.0
7.0
9.0
1.0
3.0
5.0

Figure 9

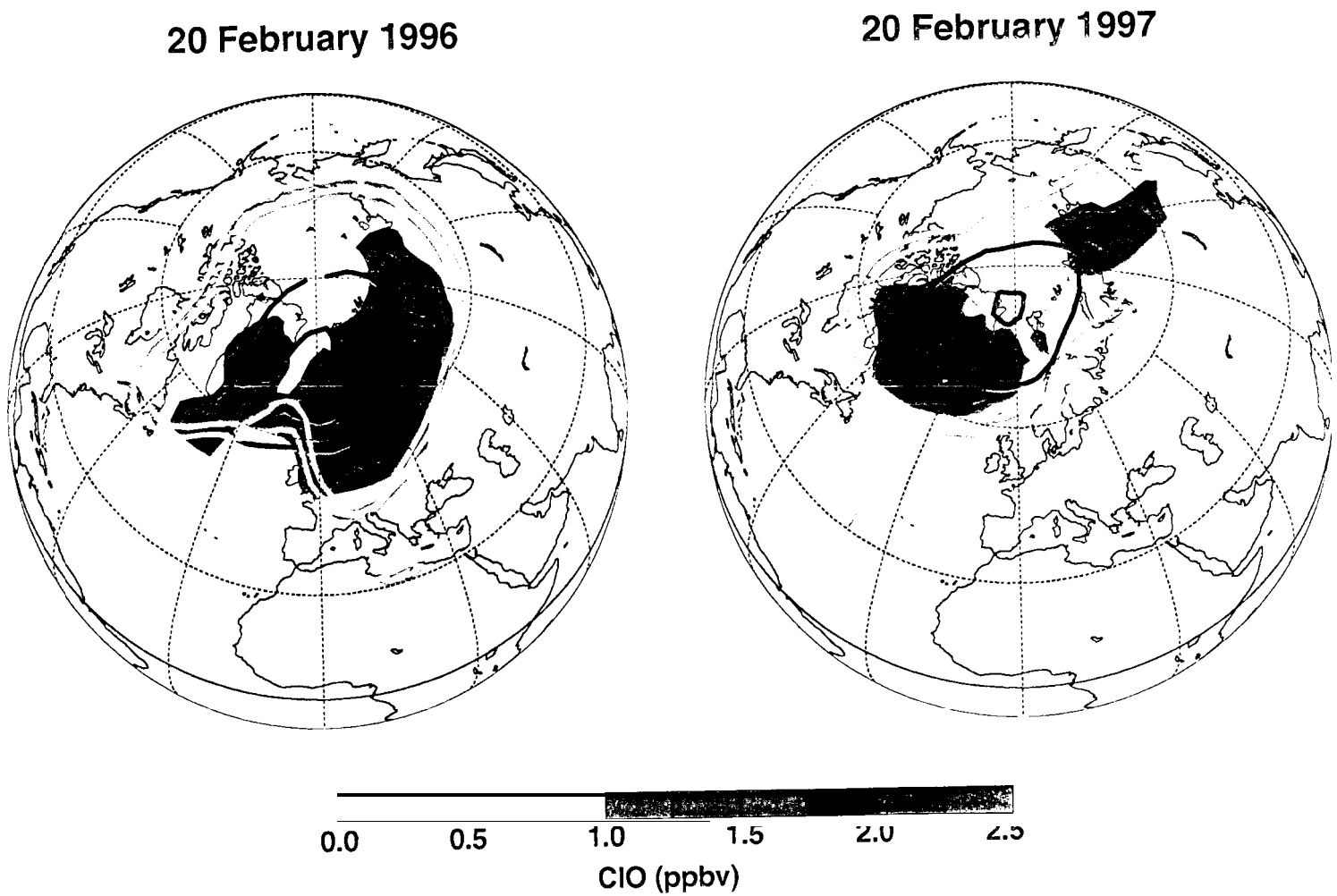

Figure 10

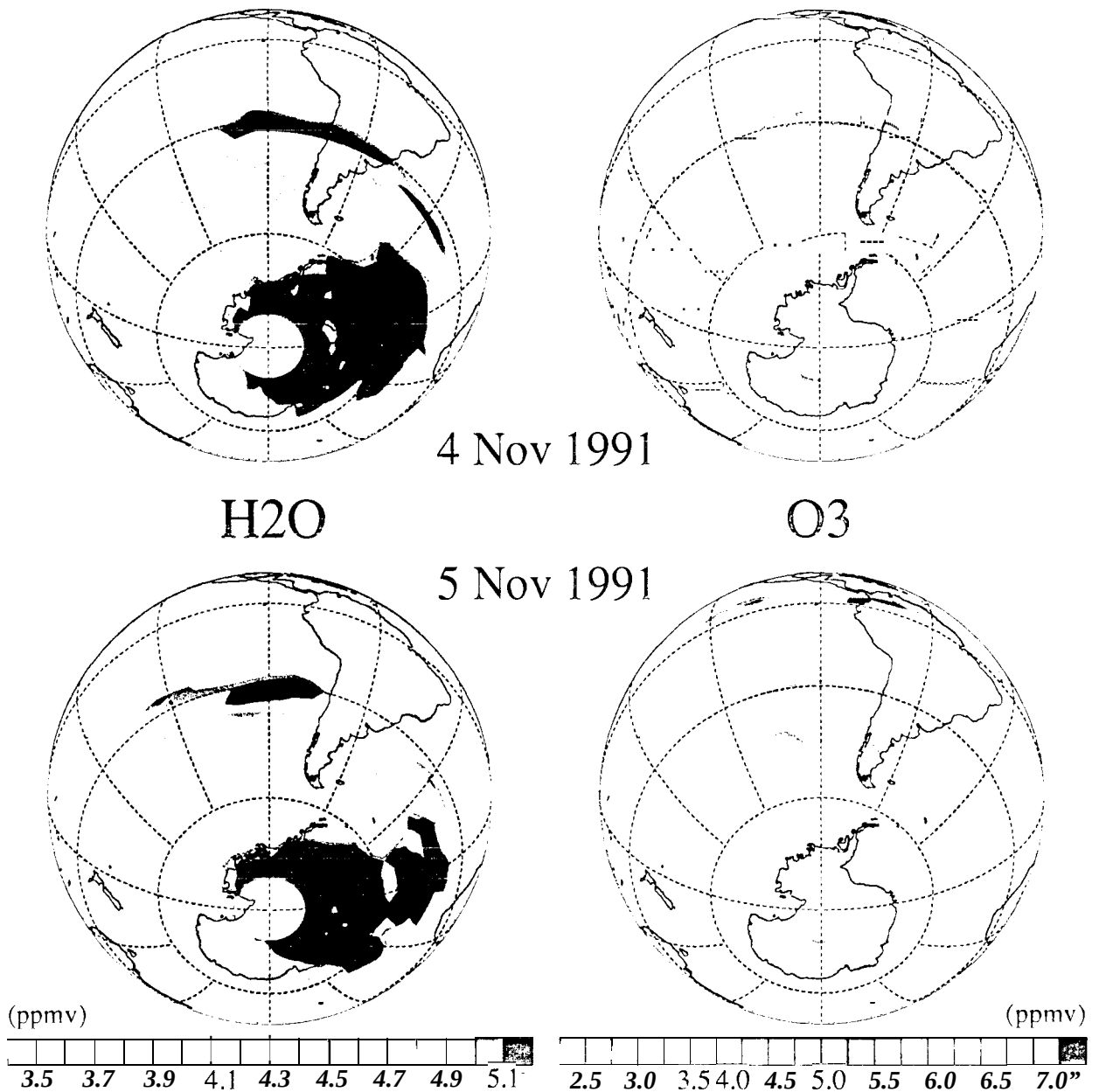
4 Nov 1991
H2O
O3
5 Nov 1991
(ppmv)
3.5 3.7 3.9 4.1 4.3 4.5 4.7 4.9 5.1
(ppmv)
2.5 3.0 3.5 4.0 4.5 5.0 5.5 6.0 6.5 7.0”

Figure 11

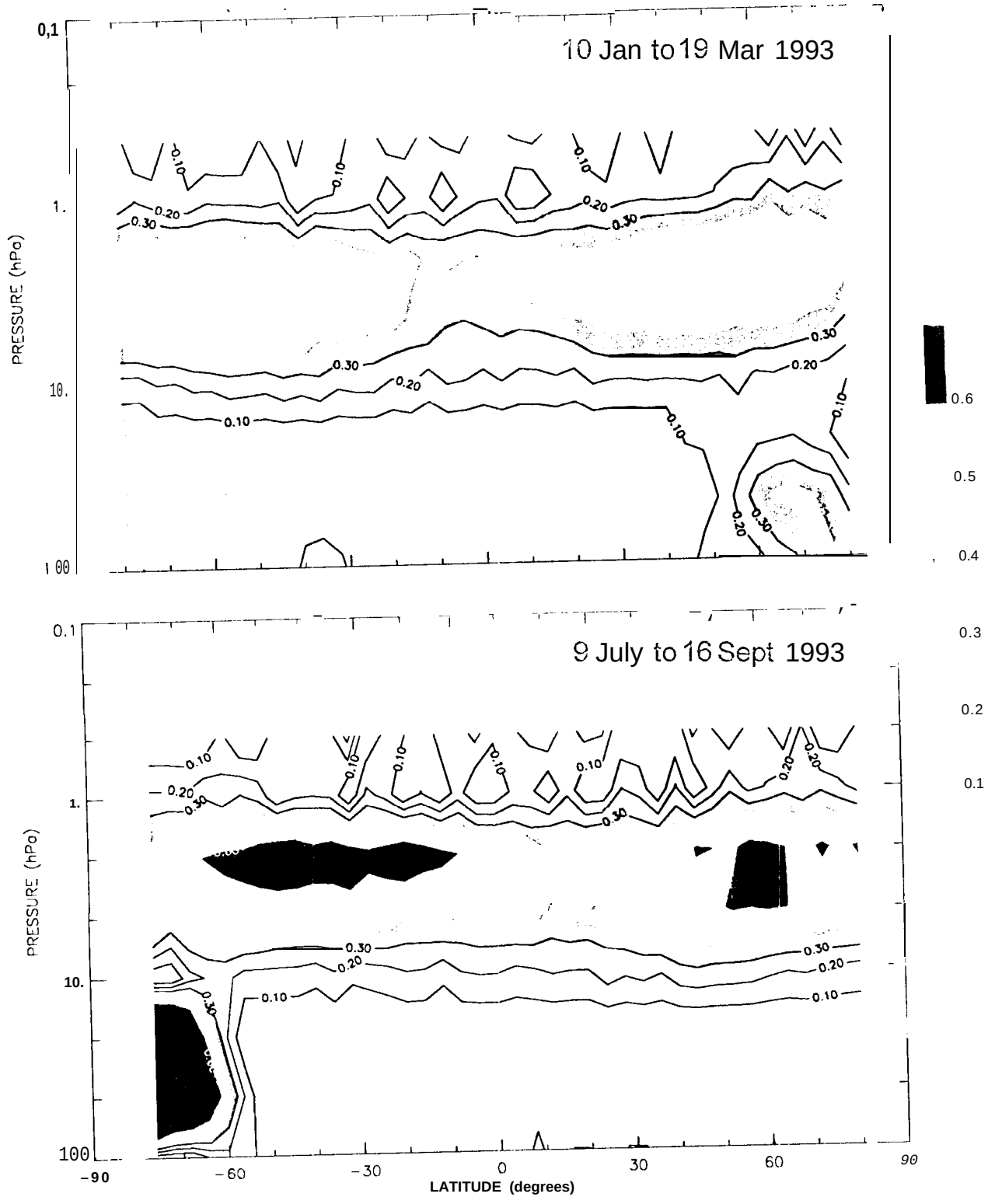
10 Jan to 19 Mar 1993
9 July to 16 Sept 1993
PRESSURE (hPa)
0,1
1.
10.
100
0.1
0.10
0.20
0.30
0.6
0.5
0.4
0.3
0.2
0.1
-90
-60
-30
0
30
60
90
LATITUDE (degrees)

Figure 12

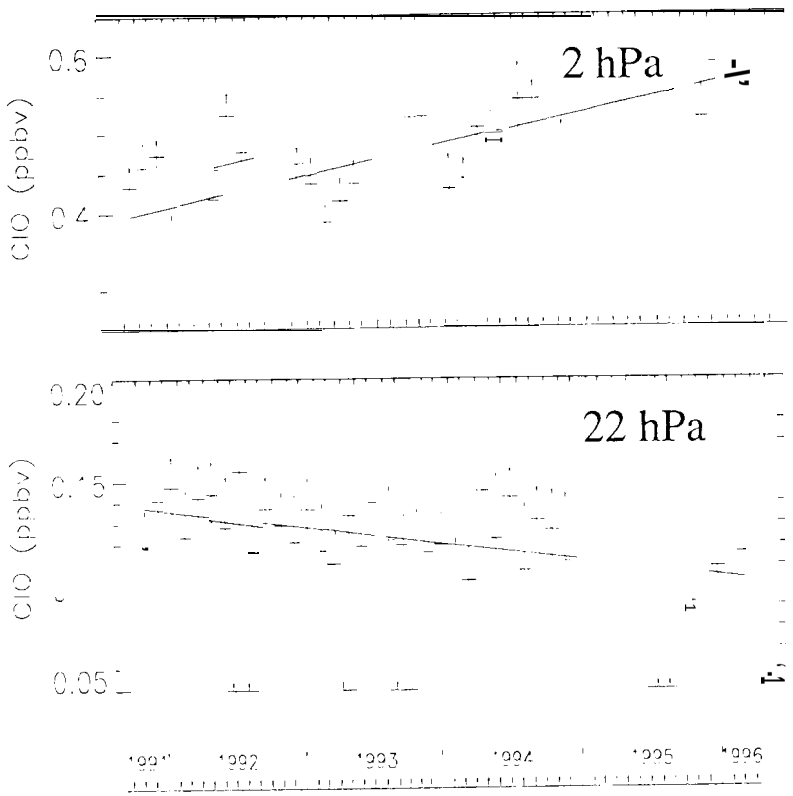
2 hPa
ClO (ppbv)
0.6
0.4
22 hPa
ClO (ppbv)
0.20
0.15
0.05
1992
1993
1994
1995
1996

Figure 3

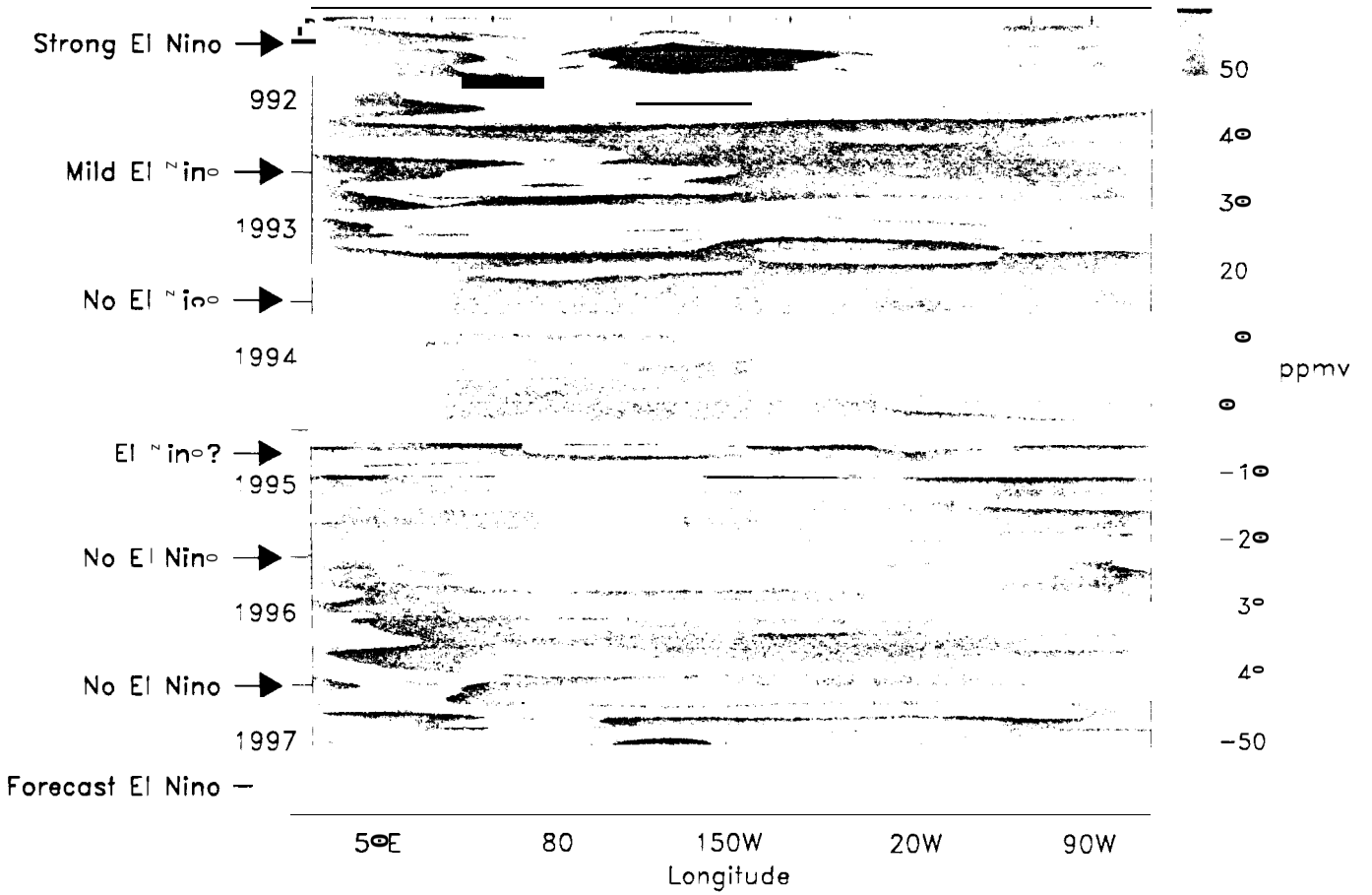
Strong El Nino
992
Mild El Nino
1993
No El Nino
1994
El Nino?
1995
No El Nino
1996
No El Nino
1997
Forecast El Nino
50
40
30
20
0
ppmv
0
-10
-20
3°
4°
-50
5°E
80
150W
20W
90W
Longitude

Figure 14

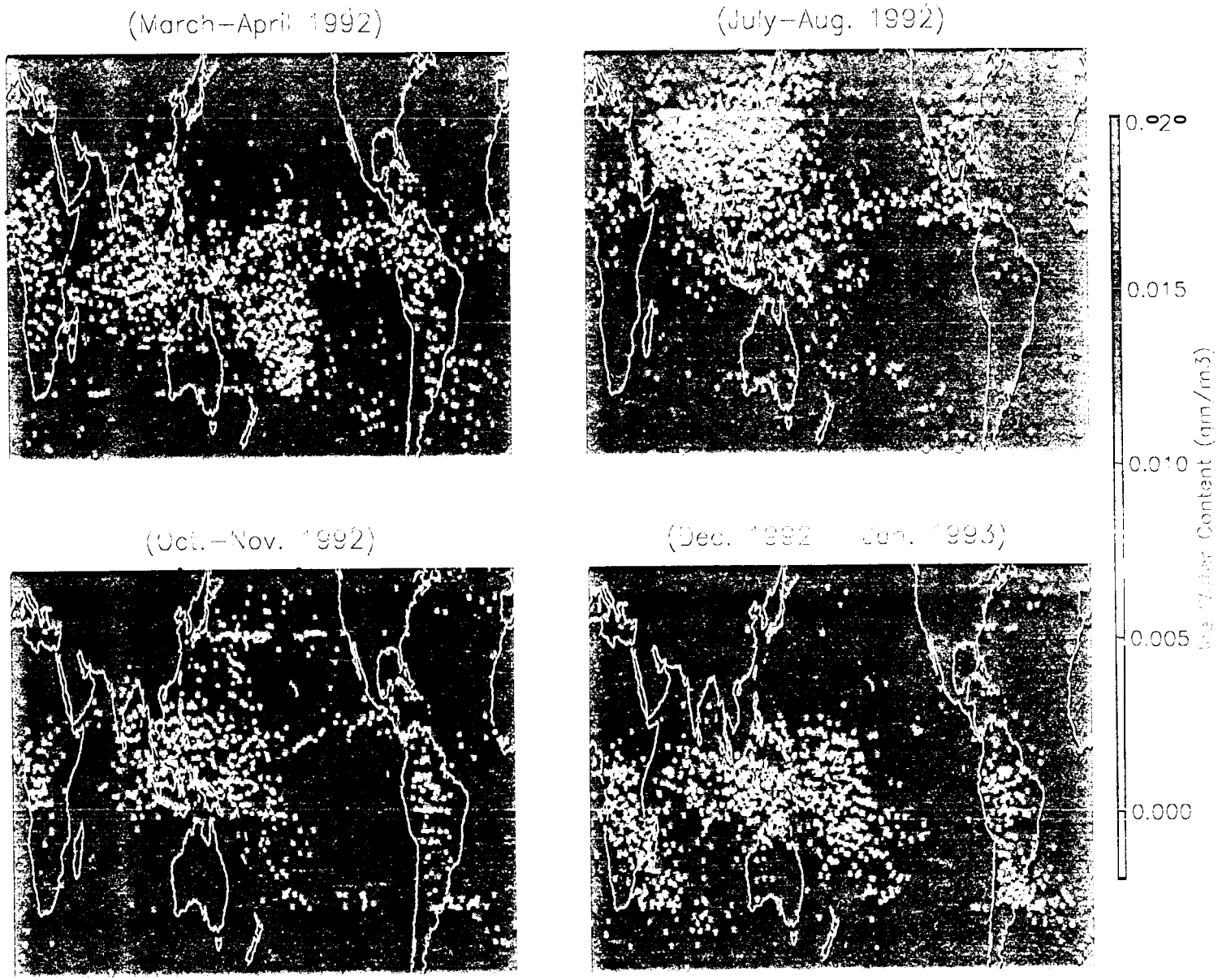
(March–April 1992)
(July–Aug. 1992)
(Oct.–Nov. 1992)
(Dec. 1992 – Jan. 1993)
0.020
0.015
0.010
0.005
0.000
Ice Water Content (gm/m3)

Figure 5

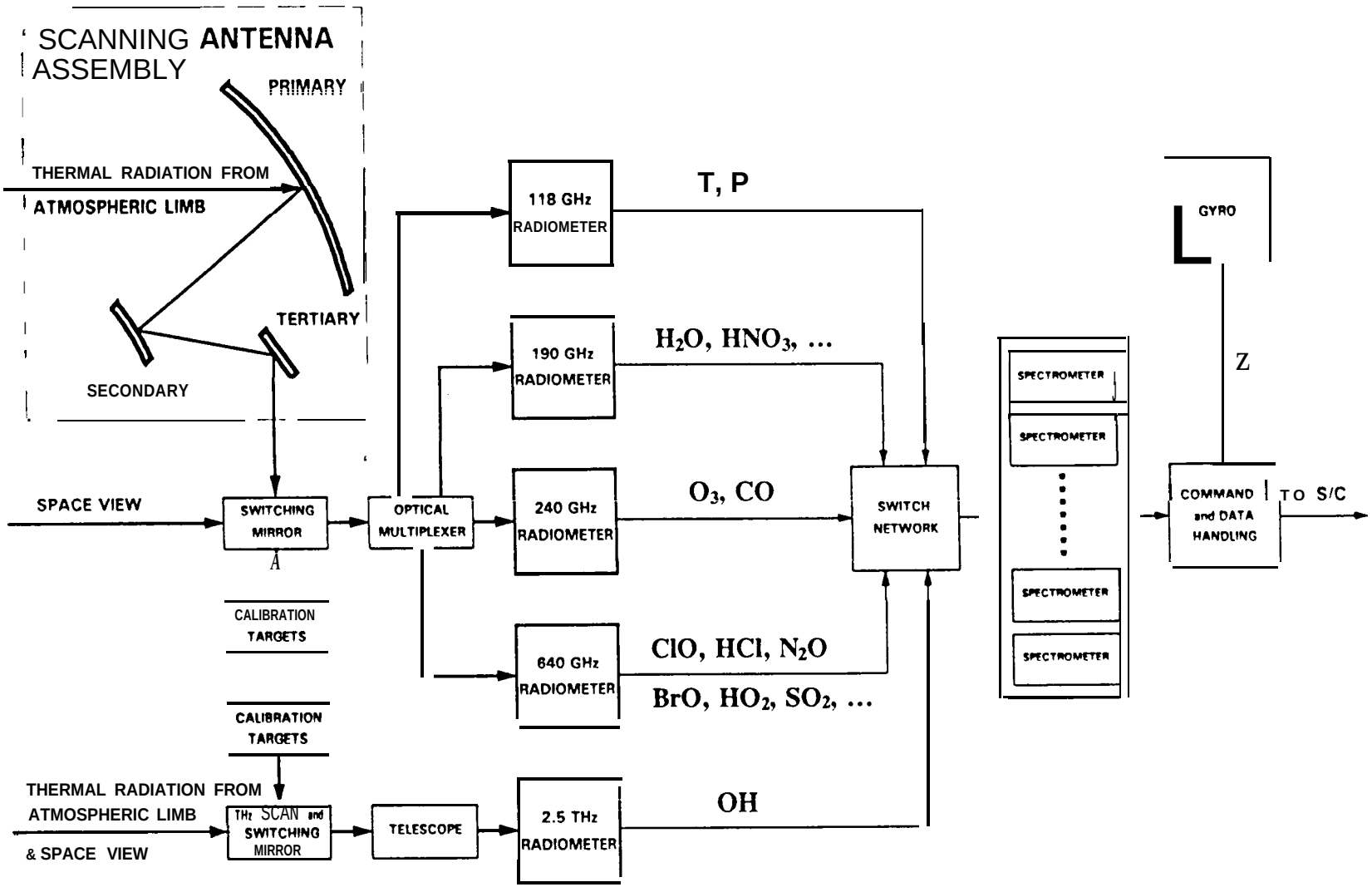
SCANNING ANTENNA ASSEMBLY
PRIMARY
THERMAL RADIATION FROM ATMOSPHERIC LIMB
TERTIARY
SECONDARY
SPACE VIEW
SWITCHING MIRROR
A
OPTICAL MULTIPLEXER
118 GHz RADIOMETER
T, P
190 GHz RADIOMETER
H_2O, HNO_3, ...
240 GHz RADIOMETER
O_3, CO
640 GHz RADIOMETER
ClO, HCl, N_2O
BrO, HO_2, SO_2, ...
SWITCH NETWORK
SPECTROMETER
SPECTROMETER
SPECTROMETER
SPECTROMETER
GYRO
Z
COMMAND and DATA HANDLING
TO S/C
CALIBRATION TARGETS
CALIBRATION TARGETS
THERMAL RADIATION FROM ATMOSPHERIC LIMB & SPACE VIEW
THz SCAN and SWITCHING MIRROR
TELESCOPE
2.5 THz RADIOMETER
OH

Figure 16

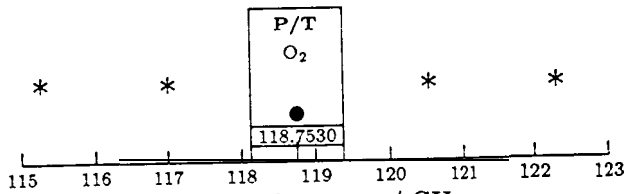
P/T
O_2
118.7530
115 116 117 118 119 120 121 122 123
Observation frequency / GHz

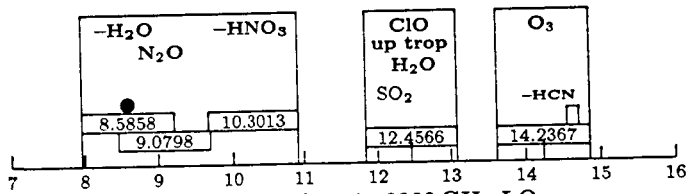
$-H_2O$ $-HNO_3$
N_2O
8.5858
9.0798
10.3013
ClO
up trop
H_2O
SO_2
12.4566
O_3
-HCN
14.2367
7 8 9 10 11 12 13 14 15 16
IF frequency for 191.9000 GHz LO

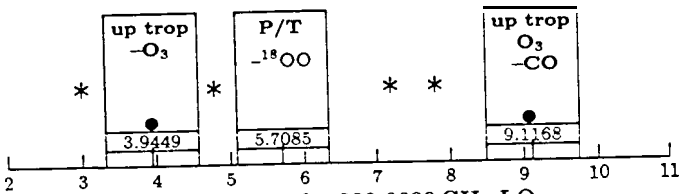
up trop
$-O_3$
3.9449
P/T
$-^{18}OO$
5.7085
up trop
O_3
$-CO$
9.1168
2 3 4 5 6 7 8 9 10 11
IF frequency for 239.6600 GHz LO

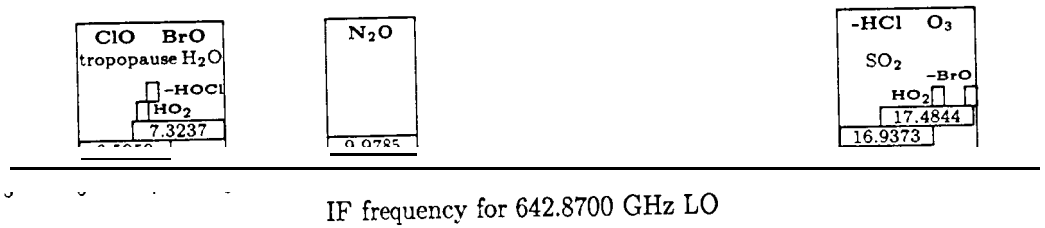
ClO BrO
tropopause H_2O
-HOCl
HO_2
7.3237
N_2O
-HCl O_3
SO_2
-BrO
HO_2
17.4844
16.9373
IF frequency for 642.8700 GHz LO

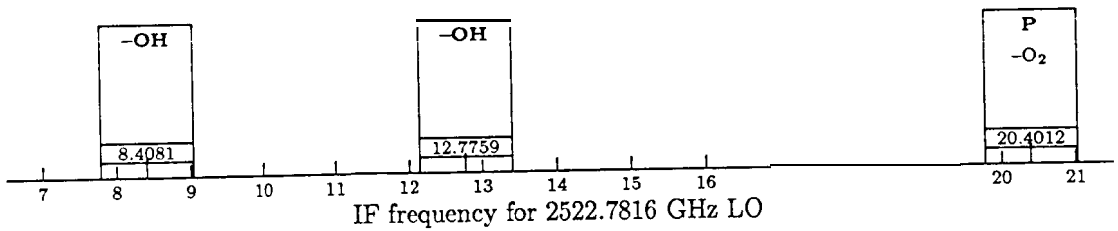
-OH
8.4081
-OH
12.7759
P
$-O_2$
20.4012
7 8 9 10 11 12 13 14 15 16 20 21
IF frequency for 2522.7816 GHz LO

Figure 7

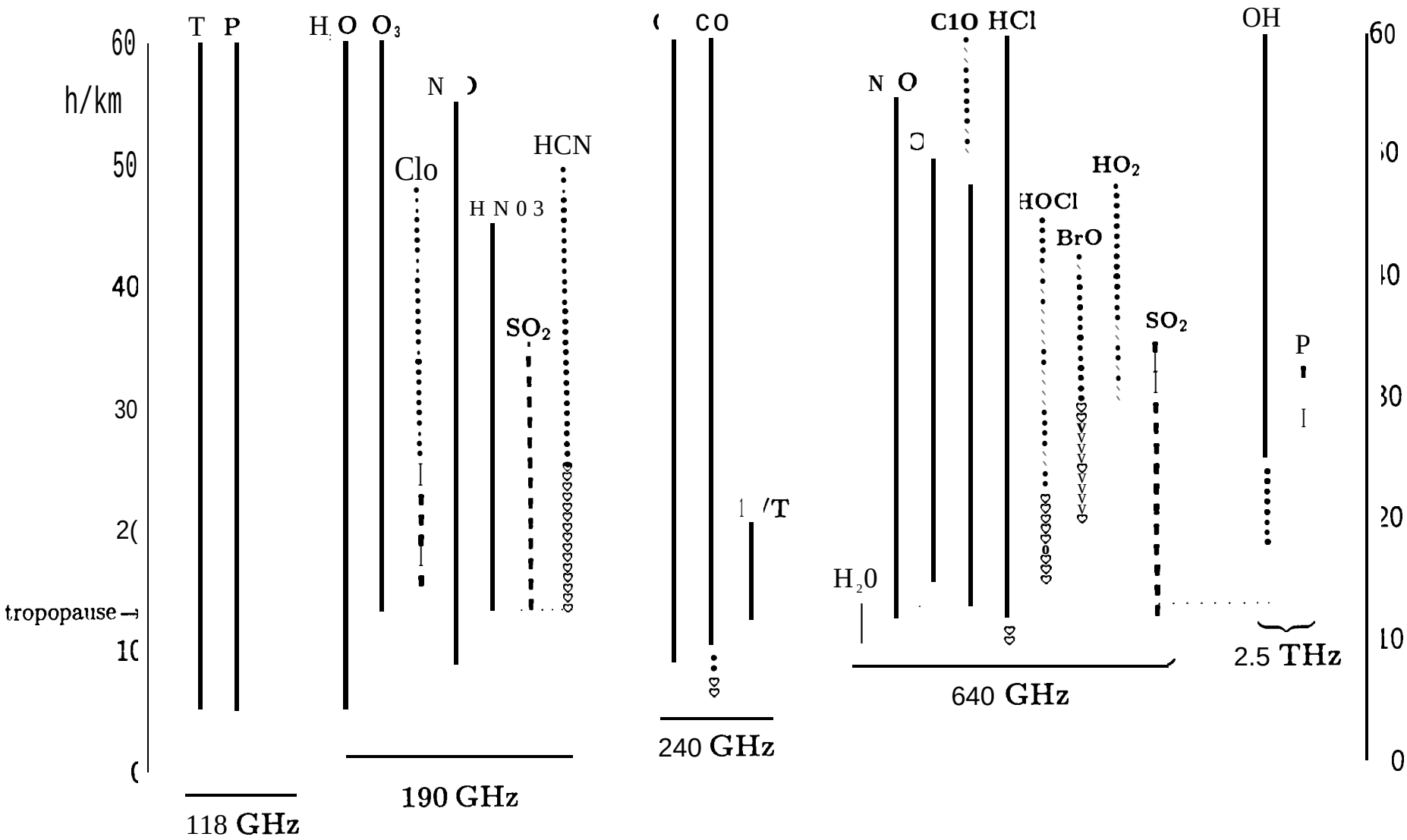
h/km
60
50
40
30
20
tropopause
10
0
T
P
H O
O3
N O
Clo
HCN
H N 0 3
SO2
118 GHz
190 GHz
CO
240 GHz
C1O
HCl
N O
H2O
HO2
HOCl
BrO
SO2
OH
P
640 GHz
2.5 THz

Figure 18